We thank reviewers for their comments on this manuscript. We have tried to address all comments, and please find our responses to comments below.

Anonymous Referee #1 comments:
Received and published: 15 July 2019

General Comments

1. The paper addresses the implication of nitrogen sources on ecosystem production in the Gulf of Mexico (GOM) and the coastal sea off Korea (CSK) using a mass-balance approach. It is generally well-written, but there are some confusing aspects. One of the aims of the study is to test a hypothesis about the controls on coastal productivity originally laid out by Rowe and Chapman (2002), which divides coastal waters into brown, green and blue zones, based on productivity. Unfortunately, figure 5 also codes stations in different subregions (each of which span these zones) using a different color scheme.

   Response: The brown-green-blue hypothesis of Rowe and Chapman is based on distance from the riverine input, as shown in Fig. 5, but for operational reasons stations were occupied in three different regions along the coast, near the Mississippi (red dots, A), an intermediate region (grey dots, B), and near the Atchafalaya (blue dots, C). To prevent a confusion, we added further explanation in the main text (lines 283-285) and caption of Fig. 5 (line 968-970), as follows:

   "For operational and modeling purposes, stations were grouped into three regions – near the Mississippi (A), near the Atchafalaya (C) and an intermediate region between ~90°-91°W."

   Added to caption of Fig. 5: "Red, grey and blue stations correspond to sub-regions A (near the Mississippi River), B (between the Mississippi and Atchafalaya), and C (near the Atchafalaya) respectively."

2. The study involves considerable data synthesis using datasets from both the GOM and CSK regions. Perhaps the reason for comparing these two regions is simply the availability of data, but the paper does not otherwise suggest why these particular regions were chosen. Is there a compelling reason to compare only Korean coastal waters with the GOM instead of broadening the comparison to include other data-rich regions (e.g. the Baltic or other European regions)? Some further explanation is required.

   Response: Thanks for the comments. We were not trying to cover the globe, and the available data were from the CSK and GOM. The main reason to compare the CSK with the GOM because of the difference in nitrogen supply via AN-D. The AN-D source is considerably larger in the CSK region than in the GOM (Wade and Sweet, 2008; Zhao et al., 2015). Comparing our results with data from other regions could be a future effort. We added further explanation in the main text (lines 22-25) as follows:

   "The GOM and CSK were selected in this study because while the major input source to the coastal ocean in both regions is riverine, the AN-D and SGD are considerably more important in the CSK region (Wade and Sweet, 2008; Zhao et al., 2015)."

3. The authors have chosen a mass-balance approach, and similar approaches have been used in many other studies. Some earlier modelling studies are cited (lines 23-26) but mass-balance approaches have been used successfully in many regions and individual coastal systems to estimate ecosystem metabolism, nutrient and carbon fluxes (e.g. the large literature generated by the LOICZ project to name a single program, as well as detailed mass balance studies of the Chesapeake Bay, the Baltic and other regions by individual research groups over the years). It seems as if the literature cited could reflect more of this earlier and ongoing work.

   Response: Thank you for your suggestions. As we mentioned above response (#2), we focused on the CSK and GOM regions in this paper, not on a global synthesis. Thus, we focused on papers that discuss the hypoxia and physical processes in the GOM and CSK (rather than those that cover estuary and riverine systems). We have added references to some mass balance model studies on other regions as you suggested in the main text (lines 31-37) as follows:

   "…and such models have been successfully used in many regions and individual coastal systems to estimate ecosystem metabolism, e.g., in the Patuxent River estuary of the Chesapeake Bay (Hagy et al. 2000; Testa et al., 2008) and in the LOICZ (Land Ocean Interactions in the Coastal Zone) project (e.g., Ramesh et al., 2015). However, there are few such model studies in the GOM and CSK. All previous models for the GOM and the CSK have considered only riverine N as the predominant input source, and no one has considered AN-D as an input in either region."

4. I found the presentation of the steady-state mass balance approach to be a little weak in that the equations inadequately representing all the terms present in each of the 3 regions being considered (2 layers for each of the red, brown, and blue subcompartments).

   Response: Our original Fig. 3a only showed each input/output terms, so we modified Fig. 3a more correctly based on reviewer's comments (each term contains several factors such as denitrification, vertical sinking etc.) as follow:

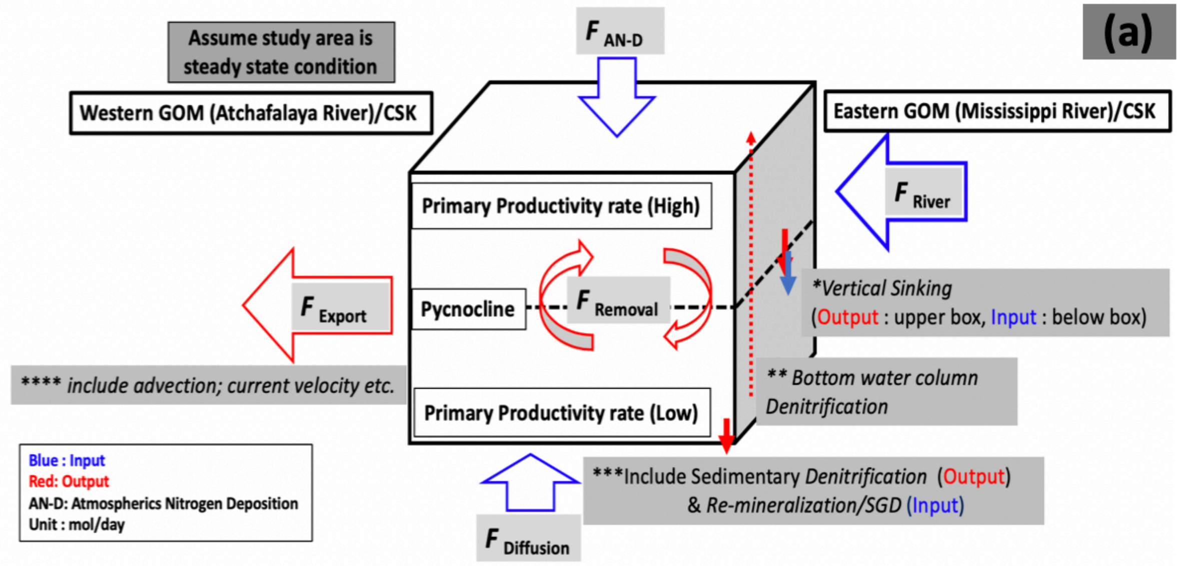

Especially, both regions have the same input/output terms although the percentages of each term are different, and both regions include sedimentary denitrification as an output factor in the sub-pycnocline layer box. This factor is included within F^{DIN}_{Bott} , which defined as net DIN release from the bottom sediment including nutrient regeneration, groundwater nutrient inputs, and an uptake of nitrate and nitrite by sedimentary denitrification. Also, denitrification from the water column in the bottom box is another significant N removal process, so we used direct measurement of the water column denitrification from the McCarthy et al., (2015) as another output term (F^{DIN}_{Deni}) for the GOM. In contrast, in the CSK, we could estimate that there is a very little water column denitrification based on the data of oxygen concentration. Thus, we only considered the sedimentary denitrification factor below the pycnocline layer in the CSK. We explain this more in responses #8 and #9. We added further explanation of each terms correctly in the main text (lines 153-277) with yellow highlights as follow:

“The N mass balance box model is modified from previous models to calculate the net removal of DIN inside each box, which represents potential primary production (PPP) (De Boer A.M. et al., 2010; Kim (G) et al., 2011) (Equation 1). In this model, DIN concentration includes ammonium (NH_4), nitrate (NO_2), and nitrite (NO_3).

$$F^{DIN}_{River} + F^{DIN}_{Atmo} + F^{DIN}_{Bott} - F^{DIN}_{Export} - F^{DIN}_{Deni} = F^{DIN}_{Removal} \quad \text{– Eq. 1}$$

where, F^{DIN}_{River}, an input term, is DIN flux from each river discharge and calculated with C^{DIN}_{Box}, the DIN concentration in each box, A_{Bott}, the bottom area of each quarter degree box, and F_{River}, river discharge rate ($C^{DIN}_{Box} \times A_{Bott} \times F_{River}$). As another input term, F^{DIN}_{Atmo} is the flux from atmospheric nitrogen deposition. F^{DIN}_{Bott}, the benthic flux is additional input term in the sub-pycnocline layer box. The one quarter degree blue boxes located closest to the Mississippi and Atchafalaya river mouths were assumed to be the only ones affected by riverine input (Figure 3b). As an output term, F^{DIN}_{Export} as an advection term was calculated from the current velocity in each region from observations (Nowlin et al., 1998a, b) and from literature data (Jacob et al., 2000; Lim et al., 2008) and the exchange between boxes from the residence time in each box. Note that water and nutrient exchange can take place through all four sides of each box, so the array is two-dimensional. F^{DIN}_{Export} for water mixing was calculated from these factors; C^{DIN}_{EX} is the difference in DIN concentration between adjacent boxes, V_S is the water volume of each box, and λ_{Mix} is the mixing rate of each box $\left(C^{DIN}_{EX} \times V_S \times \lambda_{Mix}\right)$. We used a reciprocal of the water residence time that we considered to represent horizontal mixing, i.e. dispersion. Another output term is F^{DIN}_{Deni}, denitrification process from the water column, and $F^{DIN}_{Removal}$ is removal by biological production. The details of the model definitions are given below in Table 3 and shown in Figure 3. Each arrow indicates input (blue) and output (red) terms (Figure 3). Input/output terms vary based on whether the boxes are above/below the pycnocline, while there are separate inputs from the Mississippi and Atchafalaya rivers in the GOM and Keum and Han rivers in the CSK, respectively.

In order to calculate the net removal of DIN in a box above the pycnocline layer, we used our N mass balance model in Equation 2.

$$F^{DIN}_{River} + F^{DIN}_{Atmo} - F^{DIN}_{Export} - F^{DIN}_{Sink} = F^{DIN}_{Removal} \quad \text{– Eq. 2}$$

The boxes above the pycnocline layer have two input terms: 1) $\boldsymbol{F^{DIN}_{River}}$, riverine N, which affects only a subset of boxes along the edge of each region, and 2) $\boldsymbol{F^{DIN}_{Atmo}}$, atmospheric nitrogen deposition (AN-D), which affects every box equally. The mean value of Asian data, as shown in Table 2 (Kim (JY) et al., 2010; Luo et al., 2014; Shou et al., 2018; Zhao et al., 2015), is used for $\boldsymbol{F^{DIN}_{Atmo}}$ of the CSK region, which is initially five times higher than that of the GOM (1.4 X 10^5 mol day^{-1}; Wade and Sweet, 2008). We also considered vertical sinking as an input for the sub-pycnocline layer box and as an output from the upper layer. Other possible input factors might be upwelling/downwelling processes; however, these factors are neglected in the model because both regions are shallow and close inshore (Feng et al., 2014; Lim et al., 2008) and we have no observational data on upwelling/downwelling rates. The output terms are the following: 1) $\boldsymbol{F^{DIN}_{Export}}$, the exchange rate between each box (obtained from the different N concentrations in each box and the mass transfer between them), and 2) $\boldsymbol{F^{DIN}_{Sink}}$, removal by biological production, including sinking (assuming that any other removal factors are neglected above the pycnocline). We tested the RC02 three zone hypothesis in the upper box layer, in which we can also examine the horizontal influence (horizontal extent) of the river plume based on production rates.

Below the pycnocline layer we used the revised Equation 3.

$$\boldsymbol{F^{DIN}_{Bott}} + \boldsymbol{F^{DIN}_{Sink}} - \boldsymbol{F^{DIN}_{Export}} - \boldsymbol{F^{DIN}_{Deni}} = \boldsymbol{F^{DIN}_{Removal}} \text{ – Eq. 3}$$

Equation 3 has two separate input terms; 1) The benthic flux $\boldsymbol{F^{DIN}_{Bott}}$ term contains all the potential input from the bottom sediment (defined here as net DIN release from the bottom sediment) including nutrient regeneration by bacteria, groundwater nutrient inputs, and an uptake of nitrate (NO_2^-) and nitrite (NO_3^-) mainly by sedimentary denitrification (McCarthy et al., 2015; Nunnally et al., 2014), and 2) $\boldsymbol{F^{DIN}_{Sink}}$ term as a vertical sinking from the box above the pycnocline layer, for which we used data from Qureshi (1995). The unit of $\boldsymbol{F^{DIN}_{Sink}}$ was converted to mol day^{-1} from the unit of original data (gN m^{-2} day^{-1}) with area of box (0.25 m x 0.25 m) and molar mass of N (14 g mol^{-1}).

In the GOM, benthic sediments provide excess ammonium to overlying water by regeneration processes such as remineralization (Lehrter et al., 2012; Nunnally et al., 2014; Rowe et al., 2002). Generally, there is an uptake of nitrate and nitrite mainly by sedimentary denitrification (McCarthy et al., 2015) or dissimilatory nitrate reduction to ammonium (DNRA) and assimilation by benthic microalgae (Christensen et al., 2000; Dalsgaard, 2003; Thornton et al., 2007). Due to this, net DIN flux was used as the value of $\boldsymbol{F^{DIN}_{Bott}}$, which shows DIN release from bottom sediments to overlying water column. For example, in the GOM, the sum of nitrate and nitrite fluxes to bottom sediments (e.g., May: -10.05, July -61.9, August: -48.42 μmol N m^{-2} h^{-1}) were similar or smaller than the flux of ammonium from bottom sediments (e.g., May: 203, July: 152, August: 156 μmol N m^{-2} h^{-1}) off Terrebonne bay (McCarthy et al., 2015). In the CSK, the sum of nitrate and nitrite flux to bottom sediments and ammonium flux are 0.5 ~ 1.4 mmol N m^{-2} d^{-1} and 1.3 ~ 9.6 mmol N m^{-2} d^{-1}, respectively, which indicated that excess ammonium with additional nitrate and nitrite were released from sediments in this region (Lee et al., 2012). The release of nitrate and nitrite in the CSK unlike the GOM can be estimated due to high inputs of nitrogen by groundwater in the CSK (Kim (G) et al., 2011) even though there is minor uptake of nitrate and nitrite. Diffusion from groundwater can probably be ignored in the GOM as Rabalais et al. (2002) reported that the groundwater discharge is very low in coastal Louisiana, but is likely important elsewhere and is known to be important in the CSK. Based on this, we averaged and sum the fluxes data of nitrate, nitrite, and ammonium from McCarthy et al., 2015 for the GOM and Lee et al., 2012 for the CSK, respectively, and then applied $\boldsymbol{F_{Bott}^{DIN}}$ value as 1.2 mmol N m^{-2} day^{-1} in the GOM and 6.2 mmol N m^{-2} day^{-1} in the CSK. Thus, in equation 3, the benthic flux term is calculated from existing literature results after considering all DIN fluxes as above (Lee et al., 2012; McCarthy et al., 2015), and then multiplied by the area of each box.

The output terms are; 1) $\boldsymbol{F_{Export}^{DIN}}$, the exchange rate between each box in the lower layer, and 2) $\boldsymbol{F_{Deni}^{DIN}}$, the denitrification rate from the water column. Due to high stratification at the pycnocline, upward transfer of dissolved material from the lower layer to the upper layer is assumed not to occur in our model. Also, denitrification from the water column below the pycnocline is a significant N removal process, which removes up to a maximum 68% of total N input from the Mississippi River in the GOM (McCarthy et al., 2015). As the value of $\boldsymbol{F_{Deni}^{DIN}}$ in the GOM, we used a direct measurement of denitrification rates from the McCarthy et al., (2015) in the water column (88 μmol m^{-2} h^{-1}, which converted to 2.1 mmol N m^{-2} day^{-1}) where the stations were exactly same as our sub-region A, B, and C. We assumed this applied only below the pycnocline where oxygen concentrations decrease. However, in the CSK, there is no water column denitrification data because the dissolved oxygen concentration has never been down below about 4 mg L^{-1} during our data periods. Based on this, we estimated that there is a very little water column denitrification in the CSK, so we did not count this term in the CSK. Thus, we only considered the sedimentary denitrification term for the CSK region.

Water transport in the region is generally from the east, i.e., from near the Mississippi River in Sub-region A to the west, near the Atchafalaya River in Sub-region C during non-summer periods. During summer, the winds change direction from easterly to westerly, blocking the water flow to the west (Cho et al., 1998). We calculated advection from current meter data collected during the LATEX program (Nowlin et al., 1998a, b) from April 1992 to December 1994, from which we determined U (west to east flow) and V (south to north flow) components (cm s^{-1}). Figure 4 shows the mean values of coastal ocean current velocities. The annual range of the currents is 0 to 30 cm s^{-1} for the longshore component, with standard deviation of about 8 cm s^{-1}, and 0 to 7 cm s^{-1} for the cross-shelf component, with a similar standard deviation, but these current velocities are not constant and change depending on time and day. The annual current velocities in the CSK are more affected by tidal exchange and the presence of the Yellow Sea Current, but velocities are similar to those in the GOM (Jacob et al., 2000; Lim et al., 2008). The annual range of the currents is around 0 to 28 cm s^{-1} and 0 to 7 cm s^{-1} for the cross-shelf component. Thus, we used the mean value of the current velocity for the time of year during each cruise in both the GOM and the CSK for calculating the advective flow in both alongshore and onshore/offshore directions.

To run the box model, we assumed three factors: 1) the study area is in a steady state condition, with equal input sources and outputs, 2) AN-D is evenly distributed across each area, and 3) DIN is fully utilized by phytoplankton growth in the layer above the pycnocline, so we can neglect other removal factors. However, in the layer below the pycnocline, as we mentioned above, denitrification, which leads to a main loss of DIN as nitrogen gas, is considered as another output term in Equation 3. Because we assumed that all DIN removed is fully consumed by primary production above the pynocline, we can calculate potential carbon fluxes and oxygen consumption using the Redfield ratio (C: N: O: P = 106: 16: 138: 1). The PPP can be compared with ^{14}C measurement data (Lohrenz et al., 1998, 1999; Redalje et al., 1994; Quigg et al., 2011) and dissolved oxygen data from MCH mooring C at 29° N, 92° W (4/3/2005 ~ 7/10/2005) (Bianchi et al., 2010)."

5. The equations are not well-linked to the figures illustrating processes and transport (figs 2 and 3). The only advective transport terms appears to be that associated with riverine inputs, which presumably occur only in the brown regions, or is this incorrect?

   Response: Figure 2 is taken from RC02 and shows the hypothesized physical and biochemical processes that initiate and sustain hypoxia on the Texas-Louisiana Shelf (Rowe and Chapman, 2002). Equations 1-3 are linked with figure 3a and b (GOM) and were applied in the same way to the CSK data. All four faces of each box have input/output advective terms, while the top and bottom of the upper layer include air-sea deposition and a sinking term into the bottom layer respectively. The latter is an input term for the lower layer, while sediment/water exchanges are considered across the bottom face of the lower layer. Thus, riverine input applies only to the inshore boxes in the brown zone. The term Export N (Mixing) incorporates the advective transport term between boxes in 2 dimensions. The values of advection term (F_{Export}^{DIN}) in the GOM and CSK showed similar range in the previous studies of each regions (Jacob et al., 2000; Lim et al., 2008; Nowlin et al., 1998a, b), so we applied the same value to both regions. We explained more details of advection term in the main text (lines 166-170, lines 261-266) and the caption of Fig. 3 (lines 954-960) as follows:

   "As an output term, $\boldsymbol{F_{Export}^{DIN}}$ as an advection term was calculated from the current velocity in each region from observations (Nowlin et al., 1998a, b) and from literature data (Jacob et al., 2000; Lim et al., 2008) and the exchange between boxes from the residence time in each box. Note that water and nutrient exchange can take place through all four sides of each box, so the array is two-dimensional."

   "The annual current velocities in the CSK are more affected by tidal exchange and the presence of the Yellow Sea Current, but velocities are similar to those in the GOM (Jacob et al., 2000; Lim et al., 2008). The annual range of the currents is around 0 to 28 cm s^{-1} and 0 to 7 cm s^{-1} for the cross-shelf component. Thus, we used the mean value of the current velocity for the time of year during each cruise in both the GOM and the CSK for calculating the advective flow in both alongshore and onshore/offshore directions."

   Added to caption of Fig. 3: "Export N (Mixing) represents the advective transport term. The processes of biogeochemical and transport processes of both regions are the same and each in/out put factor is the same in the GOM and CSK. Note that transfer between boxes occurs in both directions alongshore and onshore/offshore and is not a one-dimensional process as suggested in the diagram."

6. Neither layers seem to include advective terms related to upwelling, though upwelling is indicated to be important in some areas (e.g. lines 329-331). In my view, it is better to include all terms specific to each type of compartment rather than to generalize, even if more equations are needed in the text or in supplementary material (perhaps an equation for each layer in each of the blue, green and brown categories? unless they are identical). Also, the compartments appear to be treated as two-layer, 1-d longitudinal profiles instead of two 2-d layers (lateral

extent in 2 d), i.e. the implication of a grid with an upstream and downstream neighbor in open water, not 4 neighbors, one on each face of the gridcell. Can this be clarified? The units of each term in the mass balance are inconsistent, based on the definitions in table 3 (see below).

Response: We think this is a good suggestion for the future model improvement. However, given that both regions are very shallow and are generally subject to well-established pycnoclines, this suggests that in summer at least, upwelling is not very important. This agrees with a previous study in the GOM (Feng et al., 2014). We added this further explanation in the main text (lines 190-194) as follows:

"We also considered vertical sinking as an input for the sub-pycnocline layer box and as an output from the upper layer. Other possible input factors might be upwelling/downwelling processes; however, these factors are neglected in the model because both regions are shallow and close inshore (Feng et al., 2014; Lim et al., 2008) and we have no observational data on upwelling/downwelling rates."

7. It seems odd that figure 3 illustrates the biogeochemical and transport processes of regions in the GOM, but there is no analogous figure for the Korean coastal waters. Is such a figure assumed to be redundant?

   Response: Yes, we have assumed that biogeochemical and transport processes of both regions are the same, so we only illustrated the GOM region in Fig. 3. However, the importance of each term is different in the two regions. For example, AN-D occurs in both regions, but the percentage in the GOM is less than that in the CSK region (Wade and Sweet, 2008; Zhao et al., 2015). As we mentioned above response (#5), the values of advection term (F_{Export}^{DIN}) in the GOM and CSK showed similar range in the previous studies of each regions (Jacob et al., 2000; Lim et al., 2008; Nowlin et al., 1998a, b), so we applied the same value to both regions. We added this further explanation in the main text (lines 166-170, lines 261-266) and the caption of Fig. 3 (lines 954-960). Please see above response (#5).

8. The four "factors" (i.e. assumptions) necessary to run the model (lines 196-203) include the assumptions of steady state, spatial homogeneity, equivalence of biomass and primary production(!) and neglect of denitrification. These assumptions are a bit breathtaking, and at the very least require additional discussion, clarification (specifically, how is primary production rate calculated from chlorophyll measurements) and justification. The carbon equivalent of chlorophyll represents a carbon pool, not a rate of carbon production, so more is needed to estimate primary production than the chlorophyll:C ratio.

   Response: We have removed all references to EPP (calculated from the carbon:chlorophyll ratio) from the text and instead now compare our results with published ^{14}C productivity measurements and satellite-derived estimates of productivity. Actually, we considered sedimentary denitrification within the benthic flux term ($\boldsymbol{F_{Bott}^{DIN}}$) and DIN concentration includes ammonium (NH_4), nitrate (NO_2), and nitrite (NO_3) in our model. Sedimentary denitrification in the lower layer and dissimilatory nitrate reduction to ammonium (DNRA) is an important nitrogen removal process, but regeneration processes such as remineralization provides excess ammonium to overlying water (Lehrter et al., 2012; McCarthy et al., 2015;

Rowe et al., 2002). Due to this, net DIN flux was calculated and used as the value of $\boldsymbol{F_{Bott}^{DIN}}$ in the GOM and CSK, respectively. In our model, sedimentary denitrification is not shown as an output term in the equation since it is already considered inside the benthic flux factor. Denitrification from the water column in the bottom box is also another significant N removal process. Due to this, we used direct measurement of the water column denitrification from the McCarthy et al., (2015) as another output term ($\boldsymbol{F_{Deni}^{DIN}}$) and added in the Equation 3 for the GOM. In contrast, in the CSK, we could estimate that there is a very little water column denitrification based on the data of oxygen concentration. Thus, we only considered the sedimentary denitrification factor below the pycnocline layer in the CSK. We added further explanation and calculation in the main text (lines 213-236, lines 238-250) as follows:

"In the GOM, benthic sediments provide excess ammonium to overlying water by regeneration processes such as remineralization (Lehrter et al., 2012; Nunnally et al., 2014; Rowe et al., 2002). Generally, there is an uptake of nitrate and nitrite mainly by sedimentary denitrification (McCarthy et al., 2015) or dissimilatory nitrate reduction to ammonium (DNRA) and assimilation by benthic microalgae (Christensen et al., 2000; Dalsgaard, 2003; Thornton et al., 2007). Due to this, net DIN flux was used as the value of $\boldsymbol{F_{Bott}^{DIN}}$, which shows DIN release from bottom sediments to overlying water column. For example, in the GOM, the sum of nitrate and nitrite fluxes to bottom sediments (e.g., May: -10.05, July -61.9, August: -48.42 μmol N m^{-2} h^{-1}) were similar or smaller than the flux of ammonium from bottom sediments (e.g., May: 203, July: 152, August: 156 μmol N m^{-2} h^{-1}) off Terrebonne bay (McCarthy et al., 2015). In the CSK, the sum of nitrate and nitrite flux to bottom sediments and ammonium flux are 0.5 ~ 1.4 mmol N m^{-2} d^{-1} and 1.3 ~ 9.6 mmol N m^{-2} d^{-1}, respectively, which indicated that excess ammonium with additional nitrate and nitrite were released from sediments in this region (Lee et al., 2012). The release of nitrate and nitrite in the CSK unlike the GOM can be estimated due to high inputs of nitrogen by groundwater in the CSK (Kim (G) et al., 2011) even though there is minor uptake of nitrate and nitrite. Diffusion from groundwater can probably be ignored in the GOM as Rabalais et al. (2002) reported that the groundwater discharge is very low in coastal Louisiana, but is likely important elsewhere and is known to be important in the CSK. Based on this, we averaged and sum the fluxes data of nitrate, nitrite, and ammonium from McCarthy et al., 2015 for the GOM and Lee et al., 2012 for the CSK, respectively, and then applied $\boldsymbol{F_{Bott}^{DIN}}$ value as 1.2 mmol N m^{-2} day^{-1} in the GOM and 6.2 mmol N m^{-2} day^{-1} in the CSK. Thus, in equation 3, the benthic flux term is calculated from existing literature results after considering all DIN fluxes as above (Lee et al., 2012; McCarthy et al., 2015), and then multiplied by the area of each box."

"2) $\boldsymbol{F_{Deni}^{DIN}}$, the denitrification rate from the water column. Due to high stratification at the pycnocline, upward transfer of dissolved material from the lower layer to the upper layer is assumed not to occur in our model. Also, denitrification from the water column below the pycnocline is a significant N removal process, which removes up to a maximum 68% of total N input from the Mississippi River in the GOM (McCarthy et al., 2015). As the value of $\boldsymbol{F_{Deni}^{DIN}}$ in the GOM, we used a direct measurement of denitrification rates from the McCarthy et al., (2015) in the water column (88 μmol m^{-2} h^{-1}, which converted to 2.1 mmol N m^{-2} day^{-1}) where the stations were exactly same as our sub-region A, B, and C. We assumed this applied only below the pycnocline where oxygen concentrations decrease. However, in the CSK, there is no water column denitrification data because the dissolved oxygen concentration has never been down below about 4 mg L^{-1} during our data periods. Based on this, we estimated that there is a very little water column denitrification in the CSK, so we did not count this term in the CSK. Thus, we only considered the sedimentary denitrification term for the CSK region."

Even with this assumption, our model result (PPP) is similar to measured rates from ^{14}C incubation reported by Quigg et al., 2011 in the three subregions A, B, and C. In the future study, we will fully consider incubation comparison in the same station. However, at this point, our assumption and all we can do are provided and our model results based on the assumption are similar range with Actual primary production from ^{14}C incubation data from previous literature paper (Dagg et al., 2007; Lohrenz et al., 1998, 1999; Redalje et al., 1994). We added further explanation in the main text (lines 333-349, 499-511) as follows:

"Additionally, Quigg et al., (2011) pointed out that these higher PP values were affected by high riverine nutrients input from the MR that flows westward during that time period.

The actual PP ranges were similar with our model-based PPP (Figure 6). However, this was different from RC02's brown zone. This might be due to the differences between methods such as ^{14}C, our N-mass balance model, and RC02's theoretical model. Typically, RC02 assumed that the brown zone is light limited due to high sediment turbidity, but our model does not account for this and only considered DIN concentrations. Except for this, our PPP results are similar to direct productivity measurements from the ^{14}C incubations (Quigg et al., 2011). Our model result (PPP) showed the same range of values as ^{14}C incubations (e.g., Dagg et al., 2007; Lohrenz et al., 1998, 1999; Quigg et al., 2011; Redalje et al., 1994) in the three sub-regions.

Note that our model assumed all the biological uptake could be converted directly to production rates, which we considered as PPP. The PPP from cruises MCH M1 ~ M8 for samples from above the pycnocline calculated using our model is reasonable based on comparison with previous PP values (Figure 6a). The PPP ranges (0.01 ~ 5.05 gC m^{-2} day^{-1}) were similar to previous ^{14}C measurement PP values of between 0.04 ~ 5.9 gC m^{-2} day^{-1}."

"RC02 considered their model to be theoretical. In the brown zone, close to the river mouth, they assumed turbidity leads to light-limited conditions. Their results agree well with measured ^{14}C PP numbers from Quigg et al. (2011) who found the lowest integrated PP is near the MR delta mouth. However, our N mass balance model did not consider light limitation and therefore PPP in the brown zone is high. Such good agreement suggests that our model can be applied to a wide region, while ^{14}C measurements are typically conducted at a few specific points, as long as such limitations are taken into account.

In the CSK, most previous production studies focused on inshore areas such as estuaries or rivers. Our research focused for the first time on the coastal ocean off Korea. Our results explained that diverse nitrogen sources need to be recognized as potential issues for future nutrient management concerned with hypoxia, eutrophication, or other environmental issues. The agreement between our results and the pattern of production based on satellite-sensing in the CSK (Son et al., 2005), suggests that our model is reasonable."

9. The absence of consideration of denitrification, especially in regions of high N enrichment such as the Korean waters discussed here, seems strange. Also, the authors note that primary production of coastal waters is jointly controlled by nitrogen and phosphorus (first paragraph

of introduction). It would be useful to have some sense of the N:P ratios of these waters to determine whether the assumption of control of productivity by nitrogen is always reasonable, and when it breaks down.

Response: As we mentioned above response (#8), sedimentary denitrification was considered within a net DIN flux term ($\boldsymbol{F_{Bott}^{DIN}}$) and water column denitrification was added as another output term ($\boldsymbol{F_{Deni}^{DIN}}$) in our model. We added further explanation in the main text (lines 214-237, lines 239-254). Please see our answer to response (#8).

We have also added something on using N:P ratios to determine nutrient limitation. As we explain, in the coastal GOM especially near the Mississippi delta mouth, the P may be more important than N (Sylvan et al., 2006) depending on the time of year (lines 10-11). However, previous studies demonstrated that both GOM and CSK regions are N-limited most of the time (Kim (G) et al., 2011; Turner and Rabalais, 2013). Related to this, we confirmed N-limited condition in our study regions in the GOM and CSK based on plotting N against P. Minimum P concentrations were about 0.5 µM/L which suggests there was always enough P for continued phytoplankton growth. We added a new figure (Fig. 9) and further explanation in the main text (lines 471-480) as follows:

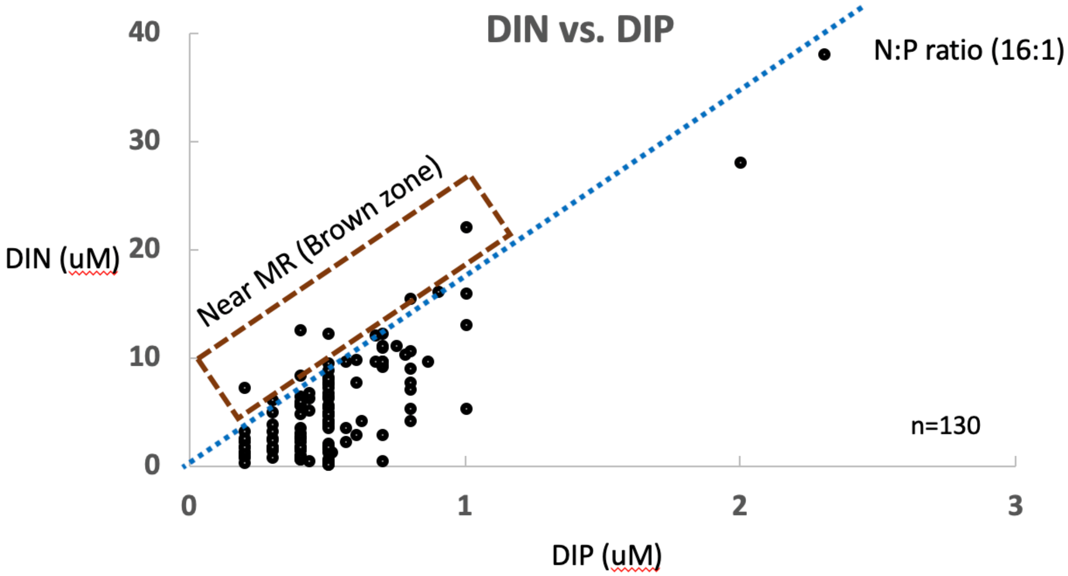

Figure 9. DIN against DIP during sampling periods in the GOM and CSK. Nearly all samples had an N:P ratio of < 16, which indicated potential N-limited condition. At a few points near the brown zone the ratio was between 16 -18; this is where light-limitation is expected according to RC02.

"Our results also agree with previous studies that demonstrated that both the GOM and CSK regions are N-limited for most of the year (Kim (G) et al., 2011; Turner and Rabalais, 2013). This compares with the results of Sylvan et al., (2007), who reported that the coastal GOM could be P-limited in the MR delta mouth area where our brown zone is located, while RC02 suggested light-limitation rather than N- or P-limitation. However, this P-limited condition appears to occur when N concentrations are very high. In particular, the N/P ratios in the both the GOM and CSK during our sampling were less than 16, indicating that both regions were N-limited, although a few stations in the brown zone near the MR river area had ratios of between 16 and 18 (Figure 9). These higher N/P ratios may result from the high sediment turbidity causing light-limited conditions in this zone near the river mouth (Rowe and Chapman, 2002)."

Specific Comments

1. The mass-balance approach used here consists of three steady-state equations for DIN removal, i.e. net inorganic N uptake associated with biological production (referred to as potential primary production; it seems like a better choice would be overall net ecosystem production). It appears that eq 1 is meant to represent a generic mass balance, and eqs 2 and 3 represent surface and bottom layers (above and below the pycnocline). Where is denitrification? Is it considered part of the sink related to FDINremoval?

   Response: Yes, Equation 1 is total consideration for upper/lower boxes and Equations 2 and 3 are applicable to the surface and bottom layers respectively. $\boldsymbol{F_{Sink}^{DIN}}$ is considered to be an output term from the upper layer and an input term for the lower layer. In the lower layer this includes contributions from both sinking and sediment-water transfer. For denitrification factor, we already considered as another output term below the pycnocline layer as we explained above. Please see our responses to #8 and #9. We added further explanation related to our assumption in the main text (lines 270-272) as follows:

   "…in the layer below the pycnocline, as we mentioned above, denitrification, which leads to a main loss of DIN as nitrogen gas, is considered as another output term in Equation 3."

2. FDINsink is obtained from sediment trap data (see table 3). Does this term (never explicitly defined in the text, but only in table 3) represent organic N particles, adsorbed DIN on mineral sediment, or both?

   Response: Yes, vertical sinking data is from Qureshi (1995). Based on her dissertation, the number represents Organic N.

3. Eqs 1-3: components of the equations are presented without units, except in table 3, and there they are inconsistent (see below #5).

   Response: When we run our model calculation, we made sure to consider the same units of factors. We have added units for all factors in Table 3. For example, to calculate the total equation 1-3, we converted the unit of $\boldsymbol{F_{Sink}^{DIN}}$ term to mol/day from gN m^{-2} day^{-1}(original data from Qureshi (1995) with area of box (0.25 x 0.25 size) and mol-N from gN using molar mass of N (14 g/mol). We added details in the caption of Table 3 (lines 1004-1007) as follows:

   Added to caption of Table 3: "** The unit of $\boldsymbol{F_{Sink}^{DIN}}$ was converted to mol day^{-1} from the unit of original data (gN m^{-2} day^{-1}) with area of box (0.25 m x 0.25 m) and molar mass of N (14 g mol $^{-1}$). All unit were converted to mol day^{-1} multiplied by area of box (0.25 m x 0.25 m)."

4. Following the development of eqs 1-3, there is some discussion of water transport in the GOM, as if the equations pertain only to this case and not the Korean waters. I think that perhaps the paper should be structured so that the conditions for each site are discussed in parallel sections, as in the Results sections. Table 2 provides estimates of atmospheric N deposition to various watersheds and water bodies from several references for different periods. It is well known that atmospheric N deposition has been declining over most of the US in recent years, and may be increasing or decreasing in Asia, depending upon the locale and period. The authors point out the difference between the increasing trends of N deposition in Korea and the decreasing or flat trends in the GOM, so it seems important to compare the two regions over the same time period. It seems like a better option (or at least a useful additional comparison) would be to include regional N deposition estimates from a global, gridded database over a common period, even if the values are generated by models. Several options exist to obtain such data, including Lamarque et al. (2013).

   Response: Please see above response (#7). We added this further explanation in the main text (main text (lines 166-170, lines 261-266) and the caption of Fig. 3 (lines 954-960). Please see above response (#5).

   Our model calculation is based on the observational data, not model simulation. Comparing our results with model simulation from previous studies could be a future effort. So, for the AN-D concentration, we have AN-D measurement data (observational data) from Sweet and Wade 2008 in the GOM and from Kim (JY) et al., 2010 in Korea. The important thing is that the AN-D concentrations are quite different in both regions (Table 2). Thus, we used different value of F_{Atmo}^{DIN} for the GOM and CSK and added further explanation in the main text (lines 187-194) and the caption of Table 3 (line 1003-1004) as follows:

   "The mean value of Asian data, as shown in Table 2 (Kim (JY) et al., 2010; Luo et al., 2014; Shou et al., 2018; Zhao et al., 2015), is used for $\boldsymbol{F_{Atmo}^{DIN}}$ of the CSK region, which is initially five times higher than that of the GOM (1.4 X 10^5 mol day^{-1}; Wade and Sweet, 2008). We also considered vertical sinking as an input for the sub-pycnocline layer box and as an output from the upper layer. Other possible input factors might be upwelling/downwelling processes; however, these factors are neglected in the model because both regions are shallow and close inshore (Feng et al., 2014; Lim et al., 2008) and we have no observational data on upwelling/downwelling rates."

   Added to caption of Table. 3: "*$\boldsymbol{F_{Atmo}^{DIN}}$ of CSK region is used as mean values of Asia data in Table 2, which is initially 5 times higher than that of GOM (1.4 X 10^5 mol day^{-1})."

5. Table 3 defines some terms not explicitly defined in the text and provides units for the terms. The units shown are not always dimensionally consistent. For example, Friver is given units of 1/days, CDINbox has units of m (1e-6 moles/l = 1e-3 moles/m3), and area has units of m2, so that the N flux associated with river input is 1e-3 moles/m/day. FDin removal has units of 1/day, which is inconsistent with this term and that of FDin atmo, which has units of mol/day. The values provided in column 3 of the table are not always in the same units as those in column 1. A good start at fixing this would be to define the units of FDin removal, preferably

in the text, and ensure that each of the terms in the equation match the units of the overall equation. Vs, the water volume of a "box" id stated to be the product of bottom area and pycnocline depth. What about the volume of the bottom layer in eq 3?

Response: As we mentioned above response (#3 of specific comments), we converted the unit of $\boldsymbol{F_{Sink}^{DIN}}$ to mol day^{-1} from the original data 0.1 ~ 1 gN m^{-2} day^{-1}. We added this explanation in the caption of Table 3 (lines 1004-1005). The volume of the bottom layer in equation 3 is area multiplied by each sampling data's pycnocline depth.

6. The comparison made between figures 6a and 8 in lines 367-373 (Lahiry's salinity-based classification vs that estimated here) is qualitative and unhelpful. Why not indicate the proportion of stations with the same classification in each period, i.e. a quantitative comparison? Rather than straining to say that there is some agreement, why not point out that there really isn't much and why. The salinity-based estimate of a large brown zone in the west in April 2004 is absent in the current estimate, and the large blue region in the center is much smaller. Why should there be much agreement given the differences in the approaches, except where the dominant driver is the massive flow of the Mississippi, which affects both salinity and nutrients? More discussion of this is warranted.

   Response: We would expect better agreement, since given that hypoxia is supposedly dependent on nitrate input, which is related to freshwater flow and stratification, even if the relationship is not simple. We revised the discussion to compare our results with previous literatures more detailed in the main text (lines 456-480) as follows:

   "Our zonal boundaries can be compared with the results of Lahiry (2007), who used salinity to define the edges of each zone for the three cruises MCH M1, M2, and M3 (Figure 8) and defined the edges of the RC02 zones in the coastal GOM based solely on salinity. Her limited simulation results indicated similar patterns to our model based on DIN concentration near the Mississippi River mouth (e.g., during MCH M1, M2, and M3). Mixing was more conservative in this region than further west because the low salinity water with high nutrients was less diluted with offshore water.

   Away from the MR in sub-regions B and C, however, her results gave very different boundaries for the three zones compared with our results (Figure 8). In particular, the results near the Atchafalaya River were very different (compare Figures 6 and 8). For example, our data showed only green and blue zones off Atchafalaya Bay during MCH M1, with no brown zone. Similarly, the extent of the blue zones in sub-region C during MCH M2 and M3 is also very different. We believe that our DIN-model based classification can cover more complex biological processes than the Lahiry (2007) method, which considers only advection and mixing and the DIN-model is a more sensible way to look at biological processes in the GOM.

   Our results also agree with previous studies that demonstrated that both the GOM and CSK regions are N-limited for most of the year (Kim (G) et al., 2011; Turner and Rabalais, 2013). This compares with the results of Sylvan et al., (2007), who reported that the coastal GOM could be P-limited in the MR delta mouth area where our brown zone is located, while RC02 suggested light-limitation rather than N- or P-limitation. However, this P-limited condition appears to occur when N concentrations are very high. In particular, the N/P ratios in the both the GOM and CSK during our sampling were less than 16, indicating that both regions were

N-limited, although a few stations in the brown zone near the MR river area had ratios of between 16 and 18 (Figure 9). These higher N/P ratios may result from the high sediment turbidity causing light-limited conditions in this zone near the river mouth (Rowe and Chapman, 2002)."

7. The differences between the above- and below-pycnocline layers are quite evident in the GOM (fig 6a,b) but not so much in the CSK. Specifically, around 90% of the grid cells in figs 7a and 7b (above and below the pycnocline) show the same classification (blue, green, brown) across all months evaluated, but less than half of the grid cells are in agreement in Fig 6a, b. Does this suggest differences in stratification in the GOM and CSK that control the homogeneity of the water column, or other factors? Again, more discussion is warranted.

   Response: We believe this is due to different amounts of freshwater flow in both regions. Typically, because the MARS provides a lot more freshwater to the GOM than the local rivers do to the CSK, we can get more stratification in the GOM than off Korea. Our model results in the CSK (Fig. 7a, b) show 90% agreement for the boxes above and below the pycnocline layer. We added further explanation in the main text (lines 400-414) as follow:

   "Around 90% of the grid cells in the CSK are in the same zones above and below the pycnocline (Figure 7 a and b) during all four cruises; however, in the GOM (Figure 6 a and b) this was found for fewer than half of the grid cells. This is probably due to the difference in freshwater discharge rate in the two regions, which leads to a much larger stratified area in the GOM than in the CSK.

   One question that has not been investigated is the temperature dependence of primary productivity in the two areas. While the GOM is temperate throughout the year, winter temperatures in the CSK fall to ~5°C. However, according to the ocean color remote sensing images from near the CSK river mouth reported by Son et al., (2005), primary production in the CSK does not appear to be strongly affected by temperature. The PPP results of our model (0.2 to 2.2 gC m^{-2} day^{-1}) agreed with their ocean color remote sensing results (0.4 to 1.6 gC m^{-2} day^{-1}) in the CSK. Also, during all seasons, the Keum River consistently supplies high amounts of DIN (average: < 60 μM) (Lim et al., 2008) to the coastal zone (especially close to the Keum mouth). We believe, therefore, that the higher value of PPP in winter near the Keum mouth (brown zone in figure 7a), is reasonable."

<u>Technical issues/typos/language</u>

1. Line 4: phosphorus is misspelled

   Response: Yes. We corrected the misspelled word (line 4).

2. Bierman et al 1994 is cited a few times in the text, but only Bierman et al 2004 appears in the references. Incorrect year?

   Response: Yes. We corrected.

3. Table 2 cites Castro and Driscoll 2002 and Castro M.S. et al. 2000. The references include a Castro et al. 2002 only.

   Response: Yes. We corrected.

4. Line 227: The PPP rate wasn't defined: : :.it is the brown zone boundary that is defined as being the region in which PPP is over the 2 g C/m2/day level: : :at least, this is my understanding. The text should be modified accordingly.

   Response: Yes. We modified the text.

References

Bianchi, T. S., DiMarco, S. F., Cowan, Jr. JH., Hetland, R. D., Chapman, P., Day, J. W., and Allison, M. A.: The Science of hypoxia in the Northern Gulf of Mexico: A review. Science of the total Environment., 408(7), 1471-1484, 2010.

Cho, K. R., Reid, O., and Nowlin, Jr W. D.: Objectively mapped stream function fields on the Texas-Louisana shelf based on 32 months of moored current meter data. Journal of Geophysics Research., 103(C5), 10377-10390, 1998.

Christensen, P. B., Rysgaard, S., Sloth, N. P., Dalsgaard, T., and Schwaerter, S.: Sediment mineralization, nutrient fluxes, denitrification and dissimilatory nitrate reduction to ammonium in an estuarine fjord with sea cage trout farms. Aquatic Microbial Ecology., 21, 73-84, 2000.

Dagg, M. J., Ammerman, J. W., AMON, R. M. W., Gardner, W. S., Green, R. E., Lohrenz, S. E.: A review of water column processes influencing hypoxia in the northern Gulf of Mexico. Estuaries Coasts., 30, 735-752, 2007.

Dalsgaard, T.: Benthic primary production and nutrient cycling in sediments with benthic microalgae and transient accumulation of macroalgae. Limnology and Oceanography., 48(6), 2138-2150, 2003.

De Boer, A. M., Watson, A. J., Edwards, N. R., and Oliver, K. I. C.: A multi-variable box model approach to the soft tissue carbon pump. Climate of the past., 6, 827-841, 2010.

Feng, Y., Fennel, K., Jackson, G. A., DiMarco, S. F., and Hetland, R. D.: A model study of the response of hypoxia to upwelling-favorable wind on the northern Gulf of Mexico shelf. Journal of Marine Systems., 131, 63-73, 2014.

Hagy, J. D., Sanford, L. P., and Boynton. W. R.: Estimation of net physical transport and hydraulic residence times for a coastal plain estuary using box models., Estuaries 23:328–340. doi:10.2307/1353325, 2000.

Jacob, G. A., Hur, H. B., and Riedlinger, S. K.: Yellow and East China Seas response to winds and currents. Journals of Geophysical Research., 105 (21), 947-968, 2000.

Kim, G., Kim, J. S., and Hwang, D. W.: Submarine groundwater discharge from oceanic islands standing in oligotrophic oceans: Implications for global production and organic carbon fluxes. Limnology and Oceanography., 56(2), 673-682, 2011.

Kim, J. Y., Ghim, Y. S., Lee, S. B., Moon, K. C., Shim, S. G., Bae, G. N., and Yoon, S. C.: Atmospheric Deposition of Nitrogen and Sulfur in the Yellow Sea Region: Significance of Long-Range Transport in East Asia. Water, Air, and Soil Pollution., 205, 259-272, 2010.

Lahiry, S.: Relationships between nutrients and dissolved oxygen concentrations on the Texas-Louisiana shelf during spring-summer of 2004. Texas A & M University. MS. Thesis., 2007.

Lee, J. S., Kim, K. H., Shim, J. H., Han, J. H., Choi, Y. H., and Khang, B. J.: Massive sedimentation of fine sediment with organic matter and enhanced benthic-pelagic coupling by an artificial dyke in semi-enclosed Chonsu Bay, Korea. Marine Pollution Bulletin., 64, 153-163, 2012.

Lehrter, J. C., Beddick Jr., D. L., Devereux, R., Yates, D. F., and Murrell. M. C.: Sediment-water fluxes of dissolved inorganic carbon, O2, nutrients, and N_2 from the hypoxic region of the Louisiana continental shelf. Biogeochemistry, 109, 233–252, 2012.

Lim, D., Kang, M. R., Jang, P. G., Kim, S. Y., Jung, H. S., Kang, Y. S., and Kang, U. S.: Water Quality Characteristics Along Mid-Western Coastal Area of Korea. Ocean and Polar Research., 30(4), 379-399, 2008.

Lohrenz, S. E., Wiesenburg, D. A., Arnone, R. A., and Chen, X. G.: What controls primary production in the Gulf of Mexico? In: Sherman K, Kumpf H, Steidinger K (ed) The Gulf of Mexico Large Marine Ecosystem: Assessment, sustainability and management. Blackwell Science, Malden, MA., 151-170, 1998.

Lohrenz, S. E., Fahnenstiel, G. L., Redalje, D. G., Lang, G. A., Dagg, M. J., Whitledge, T. E., and Dortch, Q.: Nutrients, irradiance, and mixing as factors regulating primary production in coastal waters impacted by the Mississippi River plume. Continental Shelf Research., 19, 1113-1141, 1999.

Luo, X. S., Tang, A. H., Shi, K., Wu, L. H., Li, W. Q., Shi, W. Q., Shi, X. K., Erisman, J. W., Zhang, F. S., and Liu, X. J.: Chinese coastal seas are facing heavy atmospheric nitrogen deposition. Environmental Research Letters., 9, 1-10, 2014.

McCarthy, M. J., Newell, S. E., Carini, S. A., and Cardner, W. S.: Denitrification dominates sediment nitrogen removal and is enhanced by bottom-water hypoxia in the Northern Gulf of Mexico. Estuaries and Coasts., 38, 2279-2294. 2015.

Nowlin, W. D. Jr., Jochens, A. E., Reid, R. O., and DiMarco, S. F.: Texas-Louisiana Shelf Circulation and Transport processes Study: Synthesis Report, Volume I: Technical Report. OCS Study MMS 98-0035. U.S. Dept. of the Interior, Minerals Mgmt Service, Gulf of Mexico OCS Region, New Orleans, LA., 502, 1998a.

Nowlin, W. D. Jr., Jochens, A. E., Reid, R. O., and DiMarco, S. F.: Texas-Louisiana Shelf Circulation and Transport processes Study: Synthesis Report, Volume II: Appendices. OCS Study MMS 98-0036. U.S. Dept. of the Interior, Minerals Mgmt Service, Gulf of Mexico OCS Region, New Orleans, LA., 288, 1998b.

Nunnally, C., Quigg, A., DiMarco, S. F., Chapman, P., and Rowe, G. T.: Benthic-Pelagic Coupling in the Gulf of Mexico Hypoxic Area: Sedimentary enhancement of hypoxic conditions and near bottom primary production. Continental Shelf Research., 85, 143-152, 2014.

Quigg, A., Sylvan, J., Gustafson, A., Fisher, T., Oliver, R., Tozzi, S., and Ammerman, J.: Going west: nutrient limitation of primary production in the northern Gulf of Mexico and the importance of the Atchafalaya River. Aquatic Geochemistry., 17, 519-544, 2011.

Qureshi, N. A.: The role of fecal pellets in the flux of carbon to the sea floor on a river-influenced continental shelf subject to hypoxia. Louisiana State University. Ph.D. Dissertation., 1995.

Rabalais, N. N., Turner, R. E., and Scavia, D.: Beyond science into policy: Gulf of Mexico hypoxia and the Mississippi river. Bioscience. Vol.52(2). pp.129-142, 2002.

Ramesh. R., Chen. Z., Cummins. V., Day. J., D'Elia. C., Dennison. B., Forbes. D. L., Glaeser. B., Claser. M., Clavovic. B., Kremer. H., Lange. M., Larsen. J. N., Tissier. M. Le., Newton. A., Pelling. M., Purvaja. R., and Wolanski. E.: Land-ocean interactions in the coastal zone: past, present & future, Anthtropocene., 12, 85-98, 2015.

Redalje, D. G., Lohrenz, S. E., and Fahnenstiel, G. L.: The relationship between primary production and the vertical export of particulate organic matter in a river impacted coastal ecosystem. Estuaries., 17, 829-838, 1994.

Rowe, G. T., and Chapman, P.: Continental Shelf Hypoxia: some nagging questions. Gulf Mexico Science., 20, 153-160, 2002.

Rowe, G. T., Kaegi, M. E. C., Morse, J. W., Boland, G. S., and Briones, E. G. E.: Sediment community metabolism associated with continental shelf hypoxia, northern Gulf of Mexico. Estuaries., 25(6), 1097–1106, 2002.

Shou, W., Zong, H., Ding, P., and Hou, L.: A modelling approach to assess the effects of atmospheric nitrogen deposition on the marine ecosystem in the Bohai Sea, China. Esruarine, Coastal and Shelf Science., 208, 36-48, 2018.

Son, S. H., Campbell, J. W., Dowell, M., Yoo, S. J., and Noh, J.: Primary production in the Yellow Sea determined by ocean color remote sensing. Marine Ecology Progress Series., 303, 91-103, 2005.

Sylvan, J. B., Dortch, Q., Nelson, D. M., Maier Brown, A. F., Morrison, W., Ammerman, J. W.: Phosphorus limits phytoplankton growth on the Louisiana shelf during the period of hypoxia formation. Environmental Science and Technology., 40(24), 7548– 7553, 2006.

Testa, J. M., Kemp. W. M., Boynton. W. R., and Hagy. J. D: Long-term changes in water quality and productivity in the Patuxent river estuary: 1985 to 2003. Estuaries and Coasts., 31, 1021-1037, 2008.

Thornton, D. C. O., Dong, L. F., Underwood, G. J. C., and Nedwell, D. B.: Sediment-water inorganic nutrient exchange and nitrogen budgets in the Colne Estuary, UK. Marine Ecology Progress Series., 337, 63-77, 2007.

Turner, R. E., and Rabalais, N. N.: Nitrogen and phosphorus phytoplankton growth limitation in the northern Gulf of Mexico. Aquatic microbial ecology., 68, 159–169, 2013.

Wade, T. L., and Sweet, S. T.: Final Report Coastal Bend Bays and Estuaries Program (CBBEP): Atmospheric Deposition Study., 48pp, 2008.

Zhao, Y., Zhang, L., Pan, Y., Wang, Y., Paulot, F., and Henze, D. K.: Atmospheric nitrogen deposition to the northwestern Pacific: seasonal variation and source attribution. Atmos. Chem. Phys., 15, 10905-10924, 2015.

We thank reviewers for their comments on this manuscript. We have tried to address all comments, and please find our responses to comments below.

Anonymous Referee #2 comments:
Received and published: 7 August 2019

General

1. The authors use a simple box model to estimate the potential primary production and associated oxygen demand into region, the Gulf of Mexico and Korean coastal waters. The aim and scope of the paper seem interesting and valuable for the scientific community. The method, a box model driven by observational data, is generally valid and has been used in numerous publications before. However, the authors apply several simplifying assumptions that could flaw the study: 1) DIN removal equals potential primary production – the ratio of this assumption should at least be explained and critically discussed, 2) assumption of absence of denitrification (even though at least in GOM there is large hypoxia reported). Thirdly, the hydrodynamical background of mixing between the different compartments/boxes has not been made clear. The authors should think of taking into account modelling works or extensive measuring campaigns presented in the literature in order to deliver a decent foundation for their numbers.

   Response: 1) We have addressed this point in another response (reviewer 1, #8 of general comments). The main point was to remove all references to EPP (calculated from the carbon:chlorophyll ratio) from the text and instead now compare our results with published ^{14}C productivity measurements and satellite-derived estimates of productivity. Even with this assumption, our model result (PPP) is similar to measured rates from ^{14}C incubation reported by Quigg et al., 2011 in the three subregions A, B, and C. We added further explanation in the main text (lines 333-349, 499-511) as follows:

   "Additionally, Quigg et al., (2011) pointed out that these higher PP values were affected by high riverine nutrients input from the MR that flows westward during that time period.

   The actual PP ranges were similar with our model-based PPP (Figure 6). However, this was different from RC02's brown zone. This might be due to the differences between methods such as ^{14}C, our N-mass balance model, and RC02's theoretical model. Typically, RC02 assumed that the brown zone is light limited due to high sediment turbidity, but our model does not account for this and only considered DIN concentrations. Except for this, our PPP results are similar to direct productivity measurements from the ^{14}C incubations (Quigg et al., 2011). Our model result (PPP) showed the same range of values as ^{14}C incubations (e.g., Dagg et al., 2007; Lohrenz et al., 1998, 1999; Quigg et al., 2011; Redalje et al., 1994) in the three sub-regions.

   Note that our model assumed all the biological uptake could be converted directly to production rates, which we considered as PPP. The PPP from cruises MCH M1 ~ M8 for samples from above the pycnocline calculated using our model is reasonable based on comparison with previous PP values (Figure 6a). The PPP ranges (0.01 ~ 5.05 gC m^{-2} day^{-1}) were similar to previous ^{14}C measurement PP values of between 0.04 ~ 5.9 gC m^{-2} day^{-1}."

"RC02 considered their model to be theoretical. In the brown zone, close to the river mouth, they assumed turbidity leads to light-limited conditions. Their results agree well with measured ^{14}C PP numbers from Quigg et al. (2011) who found the lowest integrated PP is near the MR delta mouth. However, our N mass balance model did not consider light limitation and therefore PPP in the brown zone is high. Such good agreement suggests that our model can be applied to a wide region, while ^{14}C measurements are typically conducted at a few specific points, as long as such limitations are taken into account.

In the CSK, most previous production studies focused on inshore areas such as estuaries or rivers. Our research focused for the first time on the coastal ocean off Korea. Our results explained that diverse nitrogen sources need to be recognized as potential issues for future nutrient management concerned with hypoxia, eutrophication, or other environmental issues. The agreement between our results and the pattern of production based on satellite-sensing in the CSK (Son et al., 2005), suggests that our model is reasonable."

Response: 2) Sedimentary denitrification was included in the bottom water boxes but was not fully explained in the text. As we mentioned in another response (reviewer 1, #8 of general comments), net DIN flux was calculated including sedimentary denitrification and regeneration process and used as the value of $\boldsymbol{F_{Bott}^{DIN}}$ in the GOM and CSK, respectively. Also, denitrification from the water column in the bottom box is another significant N removal process. Due to this, we used direct measurement of the water column denitrification from the McCarthy et al., (2015) as another output term ($\boldsymbol{F_{Deni}^{DIN}}$) and added in the Equation 3 for the GOM. However, in the CSK, we could estimate that there is a very little water column denitrification based on the data of oxygen concentration. Thus, we only considered the sedimentary denitrification factor below the pycnocline layer in the CSK. We added further explanation and calculation in the main text (lines 213-236, lines 238-250) as follows:

"In the GOM, benthic sediments provide excess ammonium to overlying water by regeneration processes such as remineralization (Lehrter et al., 2012; Nunnally et al., 2014; Rowe et al., 2002). Generally, there is an uptake of nitrate and nitrite mainly by sedimentary denitrification (McCarthy et al., 2015) or dissimilatory nitrate reduction to ammonium (DNRA) and assimilation by benthic microalgae (Christensen et al., 2000; Dalsgaard, 2003; Thornton et al., 2007). Due to this, net DIN flux was used as the value of $\boldsymbol{F_{Bott}^{DIN}}$, which shows DIN release from bottom sediments to overlying water column. For example, in the GOM, the sum of nitrate and nitrite fluxes to bottom sediments (e.g., May: -10.05, July -61.9, August: -48.42 μmol N m^{-2} h^{-1}) were similar or smaller than the flux of ammonium from bottom sediments (e.g., May: 203, July: 152, August: 156 μmol N m^{-2} h^{-1}) off Terrebonne bay (McCarthy et al., 2015). In the CSK, the sum of nitrate and nitrite flux to bottom sediments and ammonium flux are 0.5 ~ 1.4 mmol N m^{-2} d^{-1} and 1.3 ~ 9.6 mmol N m^{-2} d^{-1}, respectively, which indicated that excess ammonium with additional nitrate and nitrite were released from sediments in this region (Lee et al., 2012). The release of nitrate and nitrite in the CSK unlike the GOM can be estimated due to high inputs of nitrogen by groundwater in the CSK (Kim (G) et al., 2011) even though there is minor uptake of nitrate and nitrite. Diffusion from groundwater can probably be ignored in the GOM as Rabalais et al. (2002) reported that the groundwater discharge is very low in coastal Louisiana, but is likely important elsewhere and is known to be important in the CSK. Based on this, we averaged and sum the fluxes data of nitrate, nitrite, and ammonium from McCarthy et al., 2015 for the GOM and Lee et al., 2012 for the CSK, respectively, and then applied $\boldsymbol{F_{Bott}^{DIN}}$ value as 1.2 mmol N m^{-2} day^{-1} in the GOM and 6.2 mmol N m^{-2} day^{-1} in the CSK. Thus, in equation 3, the benthic flux term is calculated from existing literature results after considering all DIN fluxes as above (Lee et al., 2012; McCarthy et al., 2015), and then multiplied by the area of each box."

"2) $\boldsymbol{F_{Deni}^{DIN}}$, the denitrification rate from the water column. Due to high stratification at the pycnocline, upward transfer of dissolved material from the lower layer to the upper layer is assumed not to occur in our model. Also, denitrification from the water column below the pycnocline is a significant N removal process, which removes up to a maximum 68% of total N input from the Mississippi River in the GOM (McCarthy et al., 2015). As the value of $\boldsymbol{F_{Deni}^{DIN}}$ in the GOM, we used a direct measurement of denitrification rates from the McCarthy et al., (2015) in the water column (88 μmol m^{-2} h^{-1}, which converted to 2.1 mmol N m^{-2} day^{-1}) where the stations were exactly same as our sub-region A, B, and C. We assumed this applied only below the pycnocline where oxygen concentrations decrease. However, in the CSK, there is no water column denitrification data because the dissolved oxygen concentration has never been down below about 4 mg L^{-1} during our data periods. Based on this, we estimated that there is a very little water column denitrification in the CSK, so we did not count this term in the CSK. Thus, we only considered the sedimentary denitrification term for the CSK region."

Response: 3) This was not explained well in the text, but has now been corrected. The formulation of the advective terms, which are carried across all four walls of each box to give a 2-D description, rather than the 1-D shown in Fig. 3. As we mentioned in another response (reviewer 1, #5 of general comments), all four faces of each box have input/output advective terms, while the top and bottom of the upper layer include air-sea deposition and a sinking term into the bottom layer respectively. The latter is an input term for the lower layer, while sediment/water exchanges are considered across the bottom face of the lower layer. Thus, riverine input applies only to the inshore boxes in the brown zone. The term Export N (Mixing) incorporates the advective transport term between boxes in 2 dimensions. The values of advection term (F_{Export}^{DIN}) in the GOM and CSK showed similar range in the previous studies of each regions (Jacob et al., 2000; Lim et al., 2008; Nowlin et al., 1998a, b), so we applied the same value to both regions. We added this information in the main text (lines 166-170, lines 261-266) and the caption of Fig. 3 (lines 954-960) as follows:

"As an output term, $\boldsymbol{F_{Export}^{DIN}}$ as an advection term was calculated from the current velocity in each region from observations (Nowlin et al., 1998a, b) and from literature data (Jacob et al., 2000; Lim et al., 2008) and the exchange between boxes from the residence time in each box. Note that water and nutrient exchange can take place through all four sides of each box, so the array is two-dimensional."

"The annual current velocities in the CSK are more affected by tidal exchange and the presence of the Yellow Sea Current, but velocities are similar to those in the GOM (Jacob et al., 2000; Lim et al., 2008). The annual range of the currents is around 0 to 28 cm s^{-1} and 0 to 7 cm s^{-1} for the cross-shelf component. Thus, we used the mean value of the current velocity for the time of year during each cruise in both the GOM and the CSK for calculating the advective flow in both alongshore and onshore/offshore directions."

Added to caption of Fig. 3: “Export N (Mixing) represents the advective transport term. The processes of biogeochemical and transport processes of both regions are the same and each in/out put factor is the same in the GOM and CSK. Note that transfer between boxes occurs in both directions alongshore and onshore/offshore and is not a one-dimensional process as suggested in the diagram.”

Details

1. P. 10, ll. 150-152: How are ‘output terms for water mixing’ calculated in detail? Table 3 says Mix equals the ‘reciprocal of residence time’. Is this a realistic approach? In a tidal environment the work done by ‘mixing’ (dispersion would be more appropriate) increases with residence time instead of being a reciprocal. Maybe this does not apply to GOM and Korean waters but this must be described in detail (dependence of horizontal mixing, i.e. dispersion, on river run-off).

   Response: Tidal variability in the GOM is actually small (the tidal range is only ~50 cm along the northern Gulf coast) and tidal mixing in this region is considerably less than that from local currents, which are largely wind-driven (Feng et al., 2012, 2014). Reciprocal residence time has been used previously in models (e.g., De Boer A.M. et al., 2010; Kim (G) et al., 2011). Also, when we calculated the residence time factor, we already fully considered horizontal mixing based on river discharge speed, run-off, dispersion, current velocity etc. We explained more details in the revision. Please see more details in lines 170-174.

   “$\boldsymbol{F^{DIN}_{Export}}$ for water mixing was calculated from these factors; $\boldsymbol{C^{DIN}_{EX}}$ is the difference in DIN concentration between adjacent boxes, $\boldsymbol{V_S}$ is the water volume of each box, and $\boldsymbol{\lambda_{Mix}}$ is the mixing rate of each box $\left(\boldsymbol{C^{DIN}_{EX}} \times \boldsymbol{V_S} \times \boldsymbol{\lambda_{Mix}}\right)$. We used a reciprocal of the water residence time that we considered to represent horizontal mixing, i.e. dispersion.”

2. P. 10-11, ll. 160-161: How can gradient of N-concentration between boxes affect the exchange rate? N cannot drive a flow (affect equation of state).

   Response: First, we considered the difference of N-Concentrations in each box from our observational data. Then, we checked how much N concentrations were changed between each box to box. To do this, we assumed that during mixing or water flow, the changed concentration of DIN is due to the mixing factor and biological uptake.

3. P. 17, ll. 317-318: Why different threshold for ‘brown zone’ in case of GOM and CSK? “We defined” should result in one definition applying to both regions, otherwise zones can be adjusted by tuning thresholds to give geographically sound ‘results’ for each region.

   Response: We determined the threshold for each zone from our model results. There is no reason that the brown zone in each region should produce the same threshold value for PPP, since the riverine input (the main source of N in both regions) contains different DIN concentrations, while the river discharge also varies considerably. Our GOM results appear reasonable based on previous studies that defined a boundary between the green and blue zones (Dagg and Breed 2003; Lohrenz et al., 1999).

4. P. 18, l. 333: MCK or CSK, what is the correct abbreviation?

   Response: Study area in Korea is part of Mid-western CSK (coastal sea off Korea). We fixed wording CSK instead of MCK. Typically, we only used in Figure 7a, b as MCK due to area is pointed out Mid-western CSK (MCK).

5. Figure 1: Please increase font size of axis tick labels, use approximately same size for all panels.

   Response: We will fix in the final revision version.

6. Eq. 1-3: Please include units.

   Response: Yes, we put the units of the equations in the Table 3. This point was addressed this point in another response (reviewer 1, #3 of specific comments). We added details in the caption of Table 3 (lines 1004-1006) as follows:

   Added to caption of Table 3: "** The unit of $\boldsymbol{F_{Sink}^{DIN}}$ was converted to mol day^{-1} from the unit of original data (gN m^{-2} day^{-1}) with area of box (0.25 m x 0.25 m) and molar mass of N (14 g mol $^{-1}$)."

7. Figure 3: The conditions of "Export N (Mixing)" need some fundamental discussion in the text.

   Response: We have modified our original Fig. 3a to be more representative. Please see our response to reviewer 1, #4 of general comments. The term Export N (Mixing) incorporates the advective transport term between boxes in 2 dimensions. As we mentioned in above response (#1 of general, especially response 3)), the values of advection term (F_{Export}^{DIN}) in the GOM and CSK showed similar range in the previous studies of each regions (Jacob et al., 2000; Lim et al., 2008; Nowlin et al., 1998a, b), so we applied the same value to both regions. We explained more details of advection term in the main text (lines 166-170, lines 261-266) and the caption of Fig. 3 (lines 954-960).

8. Figure 4: This figure is difficult to read. Authors should think of a way to show spatial and dynamical information in one figure; for example, they could show a map of GOM (like Fig. 6) with a polar graph representing current speed and direction during one season. The current figure does not really help understand what is happening in time and space.

   Response: The current data is taken from a large program that was carried out over three years along the Texas-Louisiana shelf. We have shown the mean current speeds and their standard deviations for fortnightly intervals throughout the program. The data show clearly the change from onshore currents moving to the east during summer to generally alongshore to the west during non-summer periods. While we could have shown the data as a series of vector plots, we believe that Fig. 4 is quite comprehensible.

9. Table 4: How can EPP be higher than PPP? What does this mean?

Response: We have removed all references to EPP from the manuscript as it does not affect how the model operates and was used only for comparison with model output. Instead, we have compared our model results with spot measurements of primary production using ^{14}C and with estimates from satellite imagery.

10. Please check citation “Rowe and Chapman (2002)”. Authors seem to cite wrong title which should read “Continental Shelf Hypoxia: Some nagging questions”

    Response: Yes. I corrected.

References

Christensen, P. B., Rysgaard, S., Sloth, N. P., Dalsgaard, T., and Schwaerter, S.: Sediment mineralization, nutrient fluxes, denitrification and dissimilatory nitrate reduction to ammonium in an estuarine fjord with sea cage trout farms. Aquatic Microbial Ecology., 21, 73-84, 2000.

Dagg, M. J., and Breed, G. A.: Biological effects of Mississippi River nitrogen on the northern Gulf of Mexico-a review and synthesis. Journal of Marine Systems., 43, 133-152, 2003.

Dagg, M. J., Ammerman, J. W., AMON, R. M. W., Gardner, W. S., Green, R. E., Lohrenz, S. E.: A review of water column processes influencing hypoxia in the northern Gulf of Mexico. Estuaries Coasts., 30, 735-752, 2007.

Dalsgaard, T.: Benthic primary production and nutrient cycling in sediments with benthic microalgae and transient accumulation of macroalgae. Limnology and Oceanography., 48(6), 2138-2150, 2003.

De Boer, A. M., Watson, A. J., Edwards, N. R., and Oliver, K. I. C.: A multi-variable box model approach to the soft tissue carbon pump. Climate of the past., 6, 827-841, 2010.

Feng, Y., DiMarco, S. F., and Jackson, G. A.: Relative role of wind forcing and riverine nutrient input on the extent of hypoxia in the northern Gulf of Mexico. Geophysical Research Letters., 39, L09601, 2012.

Feng, Y., Fennel, K., Jackson, G. A., DiMarco, S. F., and Hetland, R. D.: A model study of the response of hypoxia to upwelling-favorable wind on the northern Gulf of Mexico shelf. Journal of Marine Systems., 131, 63-73, 2014.

Jacob, G. A., Hur, H. B., and Riedlinger, S. K.: Yellow and East China Seas response to winds and currents. Journals of Geophysical Research., 105 (21), 947-968, 2000.

Kim, G., Kim, J. S., and Hwang, D. W.: Submarine groundwater discharge from oceanic islands standing in oligotrophic oceans: Implications for global production and organic carbon fluxes. Limnology and Oceanography., 56(2), 673-682, 2011.

Lee, J. S., Kim, K. H., Shim, J. H., Han, J. H., Choi, Y. H., and Khang, B. J.: Massive sedimentation of fine sediment with organic matter and enhanced benthic-pelagic coupling by an artificial dyke in semi-enclosed Chonsu Bay, Korea. Marine Pollution Bulletin., 64, 153-163, 2012.

Lehrter, J. C., Beddick Jr., D. L., Devereux, R., Yates, D. F., and Murrell. M. C.: Sediment-water fluxes of dissolved inorganic carbon, O2, nutrients, and N_2 from the hypoxic region of the Louisiana continental shelf. Biogeochemistry, 109, 233–252, 2012.

Lim, D., Kang, M. R., Jang, P. G., Kim, S. Y., Jung, H. S., Kang, Y. S., and Kang, U. S.: Water Quality Characteristics Along Mid-Western Coastal Area of Korea. Ocean and Polar Research., 30(4), 379-399, 2008.

Lohrenz, S. E., Wiesenburg, D. A., Arnone, R. A., and Chen, X. G.: What controls primary production in the Gulf of Mexico? In: Sherman K, Kumpf H, Steidinger K (ed) The Gulf of Mexico Large Marine Ecosystem: Assessment, sustainability and management. Blackwell Science, Malden, MA., 151-170, 1998.

Lohrenz, S. E., Fahnenstiel, G. L., Redalje, D. G., Lang, G. A., Dagg, M. J., Whitledge, T. E., and Dortch, Q.: Nutrients, irradiance, and mixing as factors regulating primary production in coastal waters impacted by the Mississippi River plume. Continental Shelf Research., 19, 1113-1141, 1999.

McCarthy, M. J., Newell, S. E., Carini, S. A., and Cardner, W. S.: Denitrification dominates sediment nitrogen removal and is enhanced by bottom-water hypoxia in the Northern Gulf of Mexico. Estuaries and Coasts., 38, 2279-2294. 2015.

Nowlin, W. D. Jr., Jochens, A. E., Reid, R. O., and DiMarco, S. F.: Texas-Louisiana Shelf Circulation and Transport processes Study: Synthesis Report, Volume I: Technical Report. OCS Study MMS 98-0035. U.S. Dept. of the Interior, Minerals Mgmt Service, Gulf of Mexico OCS Region, New Orleans, LA., 502, 1998a.

Nowlin, W. D. Jr., Jochens, A. E., Reid, R. O., and DiMarco, S. F.: Texas-Louisiana Shelf Circulation and Transport processes Study: Synthesis Report, Volume II: Appendices. OCS Study MMS 98-0036. U.S. Dept. of the Interior, Minerals Mgmt Service, Gulf of Mexico OCS Region, New Orleans, LA., 288, 1998b.

Nunnally, C., Quigg, A., DiMarco, S. F., Chapman, P., and Rowe, G. T.: Benthic-Pelagic Coupling in the Gulf of Mexico Hypoxic Area: Sedimentary enhancement of hypoxic conditions and near bottom primary production. Continental Shelf Research., 85, 143-152, 2014.

Quigg, A., Sylvan, J., Gustafson, A., Fisher, T., Oliver, R., Tozzi, S., and Ammerman, J.: Going west: nutrient limitation of primary production in the northern Gulf of Mexico and the importance of the Atchafalaya River. Aquatic Geochemistry., 17, 519-544, 2011.

Rabalais, N. N., Turner, R. E., and Scavia, D.: Beyond science into policy: Gulf of Mexico hypoxia and the Mississippi river. Bioscience. Vol.52(2). pp.129-142, 2002.

Redalje, D. G., Lohrenz, S. E., and Fahnenstiel, G. L.: The relationship between primary production and the vertical export of particulate organic matter in a river impacted coastal ecosystem. Estuaries., 17, 829-838, 1994.

Rowe, G. T., Kaegi, M. E. C., Morse, J. W., Boland, G. S., and Briones, E. G. E.: Sediment community metabolism associated with continental shelf hypoxia, northern Gulf of Mexico. Estuaries., 25(6), 1097–1106, 2002.

Son, S. H., Campbell, J. W., Dowell, M., Yoo, S. J., and Noh, J.: Primary production in the Yellow Sea determined by ocean color remote sensing. Marine Ecology Progress Series., 303, 91-103, 2005.

Thornton, D. C. O., Dong, L. F., Underwood, G. J. C., and Nedwell, D. B.: Sediment-water inorganic nutrient exchange and nitrogen budgets in the Colne Estuary, UK. Marine Ecology Progress Series., 337, 63-77, 2007.

We thank reviewers for their comments on this manuscript. We have tried to address all comments, and please find our responses to comments below.

Anonymous Referee #3 comments:
Received and published: 11 August 2019

The manuscript applied a mass balance model based on N to two regions (GOM and CSK) with different N input source to estimate potential primary production (PPP) rate. Although similar box model has been used in many other studies, I still have some concerns about the model in this manuscript:

1. During the peak season of nutrient loading (May to July) of Mississippi-Atchafalaya River, P-limited primary production has been observed in the river plume. In the manuscript, one assumption for the box model is that "DIN is fully utilized by phytoplankton growth". Is this assumption appropriate for the brown zone in GOM? Will the model overestimate biomass in the brown zone in GOM?

   Response: Yes, it probably will. Rowe and Chapman (2002) pointed out that in the brown zone, high river discharge occurs together with high sediment loading which is likely to reduce productivity because of shading. However, as our model is estimating potential production rather than actual production in the brown zone this may not matter. This explanation is described in the main text (line 72-75) as follows:

   "They named these the brown, green, and blue zones (Figure 2). Nearest the river mouths is a 'brown' zone, where the nutrient concentrations are high, but the discharge of sediment from the river reduces light penetration and limits primary productivity within the plume."

2. Besides the nutrient and light, the temperature is another limitation for phytoplankton growth. In February, climatology SST in the CSK region is around 5 degrees celsius. As shown in Fig 7a, the brown zone has the highest PPP rate in February. I doubt very much if the model suitable for CSK region.

   Response: According to the ocean color remote sensing image near the CSK river mouth from Son et al., (2005), the results suggest that primary production in the CSK would not be limited by temperature. The PPP results of our model agreed with their ocean color remote sensing results in this region. Also, during all seasons, the Keum river consistently supplies high amounts of DIN (Lim et al., 2008) into the coastal water (especially in front of the Keum river mouth cell), and our model is of PPP based on DIN. Thus, in the Keum river mouth (brown zone in figure 7a), the higher value of PPP in the winter season is reasonable. This explanation is described in the main text (lines 405-414) as follows:

   "One question that has not been investigated is the temperature dependence of primary productivity in the two areas. While the GOM is temperate throughout the year, winter temperatures in the CSK fall to ~5°C. However, according to the ocean color remote sensing images from near the CSK river mouth reported by Son et al., (2005), primary production in the CSK does not appear to be strongly affected by temperature. The PPP results of our model

(0.2 to 2.2 gC m^{-2} day^{-1}) agreed with their ocean color remote sensing results (0.4 to 1.6 gC m^{-2} day^{-1}) in the CSK. Also, during all seasons, the Keum River consistently supplies high amounts of DIN (average: < 60 μM) (Lim et al., 2008) to the coastal zone (especially close to the Keum mouth). We believe, therefore, that the higher value of PPP in winter near the Keum mouth (brown zone in figure 7a), is reasonable."

3. The manuscript declared the current velocity data for the advective flow factor calculation in GOM but didn't for CSK.

   Response: We have addressed this point in another response (reviewer 1, #5 of general comments). CSK velocity was from Lim et al., 2008, and the range of current velocity in the CSK was similar with the range which we used in GOM. We explained more details of advection term in the main text (lines 166-170, lines 261-266) and the caption of Fig. 3 (lines 954-960) as follows:

   "As an output term, $\boldsymbol{F_{Export}^{DIN}}$ as an advection term was calculated from the current velocity in each region from observations (Nowlin et al., 1998a, b) and from literature data (Jacob et al., 2000; Lim et al., 2008) and the exchange between boxes from the residence time in each box. Note that water and nutrient exchange can take place through all four sides of each box, so the array is two-dimensional."

   "The annual current velocities in the CSK are more affected by tidal exchange and the presence of the Yellow Sea Current, but velocities are similar to those in the GOM (Jacob et al., 2000; Lim et al., 2008). The annual range of the currents is around 0 to 28 cm s^{-1} and 0 to 7 cm s^{-1} for the cross-shelf component. Thus, we used the mean value of the current velocity for the time of year during each cruise in both the GOM and the CSK for calculating the advective flow in both alongshore and onshore/offshore directions."

   Added to caption of Fig. 3: "Export N (Mixing) represents the advective transport term. The processes of biogeochemical and transport processes of both regions are the same and each in/out put factor is the same in the GOM and CSK. Note that transfer between boxes occurs in both directions alongshore and onshore/offshore and is not a one-dimensional process as suggested in the diagram."

4. The manuscript says that AD-N added N to the surface and enlarged green zone in the CSK all season. The AD-N "mainly came from" the China side. As we knew, this region is under the control of the East-Asian monsoon. If the AD-N primarily came from the China side, it should have a significant seasonal variation because of wind direction changes. Dose the AD-N input in CSK time vary? In Table 2, the authors list AN-D values from references but didn't contain AD-N they used in the model.

   Response: Not in our model. We fully agreed that AN-D in the CSK depends on wind direction, but we used the same AN-D concentration in each season because there is not enough observational data from both sides (Korea and China). Thus, at this point, all we want to say is that AN-D contributes considerably in the CSK region and this may need to be considered in future work. Based on this, we used the mean values of Asian data in table 2, which is initially 5 times higher than that of GOM. As we addressed this point in another response (reviewer 1, #4 of specific comments), we used different value of F_{Atmo}^{DIN} for the GOM and CSK and we added this information in the main text (lines 187-194) and the caption of Table 3 (lines 1003-1004) as follows:

"The mean value of Asian data, as shown in Table 2 (Kim (JY) et al., 2010; Luo et al., 2014; Shou et al., 2018; Zhao et al., 2015), is used for $\boldsymbol{F_{Atmo}^{DIN}}$ of the CSK region, which is initially five times higher than that of the GOM (1.4 X 10^5 mol day^{-1}; Wade and Sweet, 2008). We also considered vertical sinking as an input for the sub-pycnocline layer box and as an output from the upper layer. Other possible input factors might be upwelling/downwelling processes; however, these factors are neglected in the model because both regions are shallow and close inshore (Feng et al., 2014; Lim et al., 2008) and we have no observational data on upwelling/downwelling rates."

Added to caption of Table. 3: "*$\boldsymbol{F_{Atmo}^{DIN}}$ of CSK region is used as mean values of Asia data in Table 2, which is initially 5 times higher than that of GOM (1.4 X 10^5 mol day^{-1})."

5. In conclusion, "Our results agree well : : : and ocean color remote sensing in the MCK (Son et al., 2005)." Can authors add some details about the comparison in the "results" part?

   Response: This comparison is based on color remote sensing imagery from Son's paper and our predicted model results (son et al., 2010). As we mentioned above response (#2), the PPP results of our model agreed with their ocean color remote sensing results in this region (Son et al., 2010). This is described in the discussion part of revision to explain why our model is suitable in the CSK (line 405-414). Please see above response (#2).

References

Feng, Y., Fennel, K., Jackson, G. A., DiMarco, S. F., and Hetland, R. D.: A model study of the response of hypoxia to upwelling-favorable wind on the northern Gulf of Mexico shelf. Journal of Marine Systems., 131, 63-73, 2014.

Jacob, G. A., Hur, H. B., and Riedlinger, S. K.: Yellow and East China Seas response to winds and currents. Journals of Geophysical Research., 105 (21), 947-968, 2000.

Kim, J. Y., Ghim, Y. S., Lee, S. B., Moon, K. C., Shim, S. G., Bae, G. N., and Yoon, S. C.: Atmospheric Deposition of Nitrogen and Sulfur in the Yellow Sea Region: Significance of Long-Range Transport in East Asia. Water, Air, and Soil Pollution., 205, 259-272, 2010.

Lim, D., Kang, M. R., Jang, P. G., Kim, S. Y., Jung, H. S., Kang, Y. S., and Kang, U. S.: Water Quality Characteristics Along Mid-Western Coastal Area of Korea. Ocean and Polar Research., 30(4), 379-399, 2008.

Luo, X. S., Tang, A. H., Shi, K., Wu, L. H., Li, W. Q., Shi, W. Q., Shi, X. K., Erisman, J. W., Zhang, F. S., and Liu, X. J.: Chinese coastal seas are facing heavy atmospheric nitrogen deposition. Environmental Research Letters., 9, 1-10, 2014.

Nowlin, W. D. Jr., Jochens, A. E., Reid, R. O., and DiMarco, S. F.: Texas-Louisiana Shelf Circulation and Transport processes Study: Synthesis Report, Volume I: Technical Report. OCS Study MMS 98-0035. U.S. Dept. of the Interior, Minerals Mgmt Service, Gulf of Mexico OCS Region, New Orleans, LA., 502, 1998a.

Nowlin, W. D. Jr., Jochens, A. E., Reid, R. O., and DiMarco, S. F.: Texas-Louisiana Shelf Circulation and Transport processes Study: Synthesis Report, Volume II: Appendices. OCS Study MMS 98-0036. U.S. Dept. of the Interior, Minerals Mgmt Service, Gulf of Mexico OCS Region, New Orleans, LA., 288, 1998b.

Rowe, G. T., and Chapman, P.: Continental Shelf Hypoxia: some nagging questions. Gulf Mexico Science., 20, 153-160, 2002.

Shou, W., Zong, H., Ding, P., and Hou, L.: A modelling approach to assess the effects of atmospheric nitrogen deposition on the marine ecosystem in the Bohai Sea, China. Esruarine, Coastal and Shelf Science., 208, 36-48, 2018.

Son, S. H., Campbell, J. W., Dowell, M., Yoo, S. J., and Noh, J.: Primary production in the Yellow Sea determined by ocean color remote sensing. Marine Ecology Progress Series., 303, 91-103, 2005.

Wade, T. L., and Sweet, S. T.: Final Report Coastal Bend Bays and Estuaries Program (CBBEP): Atmospheric Deposition Study., 48pp, 2008.

Zhao, Y., Zhang, L., Pan, Y., Wang, Y., Paulot, F., and Henze, D. K.: Atmospheric nitrogen deposition to the northwestern Pacific: seasonal variation and source attribution. Atmos. Chem. Phys., 15, 10905-10924, 2015.

Implications of different nitrogen input sources for potential production and carbon flux estimates in the coastal Gulf of Mexico (GOM) and Korean coastal waters

Jongsun Kim,[a*] Piers Chapman,[a*] Gilbert Rowe [a, b], Steven F DiMarco [a], and Daniel Thornton [a]

[a] Department of Oceanography, Texas A&M University, College Station, TX 77843-3146, USA

[b] Department of Marine Biology, Texas A&M University, Galveston, TX 77553, USA

[*] Corresponding authors

*J. Kim. Email: jongsun@tamu.edu.

*P. Chapman. Email: piers.chapman@tamu.edu.

Submit to Ocean Sciences

Abstract

The coastal Gulf of Mexico (GOM) and Coastal Sea off Korea (CSK) both suffer from human-induced eutrophication. We used a N-mass balance model in two different regions with different nitrogen input sources to estimate organic carbon fluxes and predict future carbon fluxes under different model scenarios. The coastal GOM receives nitrogen predominantly from the Mississippi and Atchafalaya Rivers and atmospheric nitrogen deposition (AN-D) is only a minor component in this region. However, in the CSK, groundwater and atmospheric nitrogen deposition are more important controlling factors. Our model includes the fluxes of nitrogen to the ocean from the atmosphere, groundwater, and rivers, based on observational and literature data, and identifies three zones (brown, green and blue waters) in the coastal GOM and CSK with different productivity and carbon fluxes. Based on our model results, the potential primary production rate in the inner (brown water) zone are more than 2 (GOM) and 1.5 gC m^{-2} day^{-1} (CSK). In the middle (green water) zone, potential production is between 0.1 to 2 (GOM) and 0.3 to 1.5 gC m^{-2} day^{-1} (CSK). In the offshore (blue water) zone, productivity is less than 0.1 (GOM) and 0.3 (CSK) gC m^{-2} day^{-1}. Through our model scenario results, overall oxygen demand in the GOM would increase approximately 21% if we fail to reduce riverine N input, likely increasing considerably the area affected by hypoxia. Comparing the results from the U.S. with those from Korea shows the importance of considering both riverine and atmospheric inputs of nitrogen. This has direct implications for investigating how changes in energy technologies can lead to changes in the production of various atmospheric contaminants that affect air quality, climate and the health of local populations.

Keywords:

Chemical tracers, Biological processes, Shelf-seas, Gulf of Mexico, Yellow Sea.

Introduction

Industrial expansion and anthropogenic emissions are major factors leading to increased coastal productivity and potential eutrophication (Sigman and Hain 2012). Coastal primary production is controlled largely by nitrogen (N) and phosphorus (P), and the relative supply of each determines which element limits production (Paerl 2009); freshwater inputs and the distance from sources such as river mouths are also important (Dodds and Smith 2016). Changes in nutrient loading from air-borne, river-borne and groundwater sources can also affect which element limits coastal productivity (Sigman and Hain 2012). Most coastal regions are N-limited, however, at certain times conditions can change from N-limited to P-limited (Dodds and Smith 2016; Howarth and Marino 2006). Sylvan et al. (2006), for example, suggested that the coastal GOM, especially near the Mississippi River delta mouth, is P-limited at certain times.

Several studies have shown that increasing atmospheric nitrogen deposition (AN-D) is contributing to ocean production globally, including to eutrophication, and is potentially of future importance in the GOM (Cornell et al., 1995; Doney et al., 2007; Duce et al., 2008; He et al., 2010; Kanakidou et al., 2016; Kim 2018; Kim (TW) et al., 2011; Lawrence et al., 2000; Paerl et al., 2002). Recently, Kim (TW) et al. (2011), using a model simulation showed that AN-D controls approximately 52% of the coastal productivity in the Yellow Sea. Global NOx emissions have increased but appear to be changing differently in the US and Asia (Kim (JY) et al., 2010; Luo et al., 2014; Shou et al., 2018; Zhao et al., 2015), and may affect not only coastal productivity but also global total nitrogen budgets. This study uses a box model to define potential carbon fluxes based on different nitrogen input sources in two different regions, the Coastal Gulf of Mexico (GOM) and the Coastal Sea off Korea (CSK). The GOM and CSK were selected in this study because while the major input source to the coastal ocean in both regions is riverine, the AN-D and SGD are considerably more important in the CSK region (Wade and Sweet, 2008; Zhao et al., 2015).

Most previous model studies in the GOM have been used to predict the size of the hypoxic zone (e.g., Fennel et al., 2006, 2011, 2013; Green et al., 2008; Hetland and DiMarco 2008; Justic et al., 2002; Scavia et al., 2004; Turner et al. 2006, 2008), although Bierman et al. (1994), used a mass balance model to estimate carbon flux and oxygen exchange. The mass balance model is a useful tool to calculate nutrient or carbon fluxes and to estimate production in the coastal ocean (Kim (JS) et al, 2010; Kim (G) et al., 2011), and such models have been successfully used in many regions and individual coastal systems to estimate ecosystem metabolism, e.g., in the Patuxent River estuary of the Chesapeake Bay (Hagy et al. 2000; Testa et al., 2008) and in the LOICZ (Land Ocean Interactions in the Coastal Zone) project (e.g., Ramesh et al., 2015). However, there are few such model studies in the GOM and CSK. All previous models for the GOM and the CSK have considered only riverine N as the predominant input source, and no one has considered AN-D as an input in either region.

In this study, we aimed to: 1) build a mass balance model considering not only riverine N input but also air-borne and groundwater-borne N; 2) use it to calculate potential primary production in the three regions defined by Rowe and Chapman (2002, henceforth RC02, see next section) and their associated coastal productivity; and 3) use the mass balance model to test the RC02 hypothesis. Because RC02 did not quantify their model with nutrient data and no one has applied this model to another region, we tested the RC02 hypothesis using data from both the GOM and the CSK that include low salinity samples. We used historical data from the mid-western part of the CSK and evaluated the theoretical model of RC02 in both areas where freshwater with high terrestrial nutrient input mixes into the coastal ocean.

Study areas

The Texas-Louisiana (LATEX) shelf in the northern Gulf of Mexico is affected by coastal nutrient loading, leading to hypoxia, coming from two major terrestrial sources (the Mississippi and Atchafalaya Rivers that together form the Mississippi-Atchafalaya River System MARS). These two major rivers have different nutrient concentrations. The Gulf of Mexico (GOM) is a semi-enclosed oligotrophic sea and the MARS is the major source of nutrients and freshwater to the northern GOM (Alexander et al., 2008; Rabalais et al., 2002; Robertson and Saad, 2014). The MARS drains 41% of the contiguous United States (Milliman and Meade, 1983) and discharges approximately 20,000 m^3 s^{-1}, or about 60% of the total freshwater flow, (about 10.6 x 10^{11} m^3 $year^{-1}$ or 3.4 x 10^4 m^3 s^{-1}) to the northern side of the GOM. The remainder comes from other U.S. rivers, Mexico and Cuba (Nipper et al., 2004).

At the Old River Control Structure on the lower Mississippi River approximately 25% of the Mississippi River's water is diverted into the Atchafalaya River, where it mixes with the water in the Red River. The flow in the Atchafalaya River totals 30% of the total MARS flow (Figure 1a). Several projects have investigated the relationship between nutrients and the marine ecosystem, and how this leads to hypoxia in the GOM (e.g. Bianchi et al., 2010; Diaz and Rosenberg, 1995, 2008; Forrest et al., 2011; Hetland and DiMarco, 2008; Laurent et al., 2012; Quigg et al., 2011; Rabalais and Smith, 1995; Rabalais et al., 2007; Rabalais and Turner 2001; Rowe and Chapman 2002). Strong stratification due to the high freshwater discharge from the MARS, winds and nitrate concentration all affect hypoxia formation, with upwelling-favorable wind facilitating its development (Feng et al., 2012, 2014).

In the Northern GOM, the major factor controlling coastal productivity is riverine N input.

Rowe and Chapman (2002), defined three theoretical zones over the LATEX shelf close to the Mississippi and Atchafalaya River mouths to predict the effects of nutrient loading on hypoxia along the river plumes and over the shelf. They named these the brown, green, and blue zones (Figure 2). Nearest the river mouths is a 'brown' zone, where the nutrient concentrations are high, but the discharge of sediment from the river reduces light penetration and limits primary productivity within the plume. Further away from the river plume is a stratified 'green' zone with available light and nutrients that result in high productivity. In this region, the rapid depletion of nutrients is due to biological uptake processes that depend on the season and river flow (Bode and Dortch, 1996; Dortch and Whitledge, 1992; Lohrenz et al., 1999; Turner and Rabalais, 1994). Still further offshore, and also along the river plume to the west, there is the so-called 'blue' zone, defined arbitrarily by nitrate concentrations of 1 μM L^{-1} or less, which is dominated by intense seasonal stratification and a strong pycnocline, so that in the surface layer nutrients are limiting at this distance from the rivers and most primary production is fueled by recycled nutrients (Dortch and Whitledge, 1992). It is important to note that RC02 makes clear that the edges of the zones (geographical regimes) are not static, but change over time depending on season, river flow, and biological processes (Figure 2).

The coastal sea off western Korea (CSK) forms the eastern side of another semi-enclosed basin (the Yellow Sea) and is affected by freshwater discharge from river plumes in the same way as the coastal GOM, although the freshwater flow is considerably less. The Yellow Sea covers about 380,000 km^2 area with an average water depth of 44 m, and numerous islands are located on its eastern side (Liu et al., 2003). Our specific study area is the mid-western coastal region from the Taean Peninsula to Gomso Bay (Figures 1c and 1d).

There is a strong tidal front in the coastal area near the Taean Peninsula due to sea floor topography and the coastal configuration (Park, 2017; Park et al., 2017). The region also contains several bays (Garolim Bay, Gomso Bay and Cheonsu Bay), and is affected by discharges from a large artificial lake (Saemangeum lake) as well as the freshwater discharge from the Keum river plume that contains high concentrations of nutrients (Lim et al., 2008). Conditions in the mid-western CSK near the Taean peninsula are similar to the coastal GOM, because of mixing of two different water masses from Gyunggi Bay (Han River) and the Keum River (Choi et al., 1998, 1999). The annual mean flow rates within the Keum River were about 70 m^3 s^{-1} (normal period) and 170 m^3 s^{-1} (flood period) (Yang and Ahn 2008). Precipitation within the catchment was 1,208 mm $year^{-1}$ during 2003 to 2005 (Yang and Ahn 2008).

Unlike the coastal GOM, the CSK has increased nitrogen inputs from atmospheric nitrogen deposition (AN-D, which is approximately five times higher than in the GOM, Table 2) (Kim (JY) et al., 2010; Luo et al., 2014; Shou et al., 2018; Zhao et al., 2015) and nutrient inputs from the groundwater discharge (Kim (JS) et al., 2010; Kim (G) et al., 2011). AN-D has increased in the CSK owing to industrial development in China during the last few decades, which has led to increased atmospheric N emission.

Data and Methods

Riverine N data

Hydrographic data from the MCH (Mechanisms Controlling Hypoxia – MCH Atlas) projects in the Gulf of Mexico were collected from the National Oceanographic Data Center (https://www.nodc.noaa.gov) covering the period from 2004 through 2007 (Table 1). We excluded cruises MCH M6 and M7 because the threat of hurricanes led to sampling stations in different areas from the other cruises. The study sites and sampling areas are shown in Figure

1b. Quality control removed inconsistencies and anomalies in the data (e.g., removing outliers, missing data interpolation). Hydrographic data from the CSK (nutrients, salinity, oxygen) were collected during several cruises (Table 1 and Figure 1c and 1d), and the data were put through similar QA/QC routines.

Atmospheric Nitrogen Deposition (AN-D) data

AN-D data from around the US are sparse (Table 2). Most US data have been collected along the east coast of the US and the only data in the GOM region were collected near Corpus Christi (~10 kg/ha/year; Wade and Sweet, 2008), Considerable AN-D could be expected, however, from the large number of petrochemical and fertilizer plants in southern TX, especially near Houston and along the Mississippi. While there are more data from the Yellow Sea (Kim (JY) et al., 2010; Luo et al., 2014; Shou et al., 2018; Zhao et al., 2015), they are still limited owing to the broad sampling coverage. While AN-D data in the Asian region were up to 140 kg/ha/year, data from the eastern side of the US were under 10 Kg/ha/year, even lower than in the GOM, suggesting there is currently not a large contribution from AN-D to total N loads to the North Atlantic Ocean. The approximate order of magnitude difference in AN-D concentrations between the GOM and the CSK is due to the continuing industrial development in East Asia and the resulting N emissions (Wang et al., 2016; Zhao et al., 2015). Lamarque et al., (2013) reported model results, which covers our study regions, and their model appears to underestimate AN-D at the sampling sites compared with observational data in the GOM (Wade and Sweet, 2008). However, the pattern of AN-D inputs between GOM and CSK from Lamarque et al., (2013) shows around five times difference between the two regions, which agrees with our data. Thus, in our model, we used observational data for both regions, as shown in Table 2.

Methodology: N-mass balance model

Our model consists of three sub-regions based on sampling locations during MCH cruises (Figure 3), each of which contains a series of one-quarter degree square boxes, as followed by Belabbassi (2006). The quarter degree boxes in this study were separated into an upper box and a lower box, based on pycnocline depth, as defined by a sharp change in density and coincides generally with a minimum change in oxygen concentration of 0.5 ml/L. We assume steady state conditions, and estimate potential production, which we count as an estimate of potential carbon flux (Figure 3a). Primary production (PP) above the pycnocline is expected to be higher than below it (Anderson 1969; Sigman and Hain, 2012), which means that the two layers have different biological processes. The difference in PP between upper and lower boxes also depends on the freshwater discharge rate, which determines nutrient input to the upper layer, seasonal variability, and transfer processes between the layers. While chlorophyll can be found below the pycnocline (DiMarco and Zimmerle, 2017).

The N mass balance box model is modified from previous models to calculate the net removal of DIN inside each box, which represents potential primary production (PPP) (De Boer A.M. et al., 2010; Kim (G) et al., 2011) (Equation 1). In this model, DIN concentration includes ammonium (NH$_4$), nitrate (NO$_2$), and nitrite (NO$_3$).

$$\boldsymbol{F^{DIN}_{River}} + \boldsymbol{F^{DIN}_{Atmo}} + \boldsymbol{F^{DIN}_{Bott}} - \boldsymbol{F^{DIN}_{Export}} - \boldsymbol{F^{DIN}_{Deni}} = \boldsymbol{F^{DIN}_{Removal}} \quad \text{– Eq. 1}$$

where, $\boldsymbol{F^{DIN}_{River}}$, an input term, is DIN flux from each river discharge and calculated with $\boldsymbol{C^{DIN}_{Box}}$, the DIN concentration in each box, $\boldsymbol{A_{Bott}}$, the bottom area of each quarter degree box, and

F_{River}, river discharge rate $(C_{Box}^{DIN} \times A_{Bott} \times F_{River})$. As another input term, F_{Atmo}^{DIN} is the flux from atmospheric nitrogen deposition. F_{Bott}^{DIN}, the benthic flux is additional input term in the sub-pycnocline layer box. The one quarter degree blue boxes located closest to the Mississippi and Atchafalaya river mouths were assumed to be the only ones affected by riverine input (Figure 3b). As an output term, F_{Export}^{DIN} as an advection term was calculated from the current velocity in each region from observations (Nowlin et al., 1998a, b) and from literature data (Jacob et al., 2000; Lim et al., 2008) and the exchange between boxes from the residence time in each box. Note that water and nutrient exchange can take place through all four sides of each box, so the array is two-dimensional. F_{Export}^{DIN} for water mixing was calculated from these factors; C_{EX}^{DIN} is the difference in DIN concentration between adjacent boxes, V_S is the water volume of each box, and λ_{Mix} is the mixing rate of each box $\left(C_{EX}^{DIN} \times V_S \times \lambda_{Mix}\right)$. We used a reciprocal of the water residence time that we considered to represent horizontal mixing, i.e. dispersion. Another output term is F_{Deni}^{DIN}, denitrification process from the water column, and $F_{Removal}^{DIN}$ is removal by biological production. The details of the model definitions are given below in Table 3 and shown in Figure 3. Each arrow indicates input (blue) and output (red) terms (Figure 3). Input/output terms vary based on whether the boxes are above/below the pycnocline, while there are separate inputs from the Mississippi and Atchafalaya rivers in the GOM and Keum and Han rivers in the CSK, respectively.

In order to calculate the net removal of DIN in a box above the pycnocline layer, we used our N mass balance model in Equation 2.

$$F_{River}^{DIN} + F_{Atmo}^{DIN} - F_{Export}^{DIN} - F_{Sink}^{DIN} = F_{Removal}^{DIN} \quad \text{– Eq. 2}$$

The boxes above the pycnocline layer have two input terms: 1) F_{River}^{DIN}, riverine N, which affects only a subset of boxes along the edge of each region, and 2) F_{Atmo}^{DIN}, atmospheric nitrogen deposition (AN-D), which affects every box equally. The mean value of Asian data, as shown in Table 2 (Kim (JY) et al., 2010; Luo et al., 2014; Shou et al., 2018; Zhao et al., 2015), is used for F_{Atmo}^{DIN} of the CSK region, which is initially five times higher than that of the GOM (1.4 X 10^5 mol day^{-1}; Wade and Sweet, 2008). We also considered vertical sinking as an input for the sub-pycnocline layer box and as an output from the upper layer. Other possible input factors might be upwelling/downwelling processes; however, these factors are neglected in the model because both regions are shallow and close inshore (Feng et al., 2014; Lim et al., 2008) and we have no observational data on upwelling/downwelling rates. The output terms are the following: 1) F_{Export}^{DIN}, the exchange rate between each box (obtained from the different N concentrations in each box and the mass transfer between them), and 2) F_{Sink}^{DIN}, removal by biological production, including sinking (assuming that any other removal factors are neglected above the pycnocline). We tested the RC02 three zone hypothesis in the upper box layer, in which we can also examine the horizontal influence (horizontal extent) of the river plume based on production rates.

Below the pycnocline layer we used the revised Equation 3.

$$F_{Bott}^{DIN} + F_{Sink}^{DIN} - F_{Export}^{DIN} - F_{Deni}^{DIN} = F_{Removal}^{DIN} \quad \text{– Eq. 3}$$

Equation 3 has two separate input terms; 1) The benthic flux F_{Bott}^{DIN} term contains all the potential input from the bottom sediment (defined here as net DIN release from the bottom sediment) including nutrient regeneration by bacteria, groundwater nutrient inputs, and an uptake of nitrate (NO_2^-) and nitrite (NO_3^-) mainly by sedimentary denitrification (McCarthy et al., 2015; Nunnally et al., 2014), and 2) $\boldsymbol{F_{Sink}^{DIN}}$ term as a vertical sinking from the box above the pycnocline layer, for which we used data from Qureshi (1995). The unit of $\boldsymbol{F_{Sink}^{DIN}}$ was converted to mol day^{-1} from the unit of original data (gN m^{-2} day^{-1}) with area of box (0.25 m x 0.25 m) and molar mass of N (14 g mol^{-1}).

In the GOM, benthic sediments provide excess ammonium to overlying water by regeneration processes such as remineralization (Lehrter et al., 2012; Nunnally et al., 2014; Rowe et al., 2002). Generally, there is an uptake of nitrate and nitrite mainly by sedimentary denitrification (McCarthy et al., 2015) or dissimilatory nitrate reduction to ammonium (DNRA) and assimilation by benthic microalgae (Christensen et al., 2000; Dalsgaard, 2003; Thornton et al., 2007). Due to this, net DIN flux was used as the value of $\boldsymbol{F_{Bott}^{DIN}}$, which shows DIN release from bottom sediments to overlying water column. For example, in the GOM, the sum of nitrate and nitrite fluxes to bottom sediments (e.g., May: -10.05, July -61.9, August: -48.42 μmol N m^{-2} h^{-1}) were similar or smaller than the flux of ammonium from bottom sediments (e.g., May: 203, July: 152, August: 156 μmol N m^{-2} h^{-1}) off Terrebonne bay (McCarthy et al., 2015). In the CSK, the sum of nitrate and nitrite flux to bottom sediments and ammonium flux are 0.5 ~ 1.4 mmol N m^{-2} d^{-1} and 1.3 ~ 9.6 mmol N m^{-2} d^{-1}, respectively, which indicated that excess ammonium with additional nitrate and nitrite were released from sediments in this region (Lee et al., 2012). The release of nitrate and nitrite in the CSK unlike the GOM can be estimated due to high inputs of nitrogen by groundwater in the CSK (Kim (G) et al., 2011) even though there is minor uptake of nitrate and nitrite. Diffusion from groundwater can probably be ignored in the GOM as Rabalais et al. (2002) reported that the groundwater discharge is very low in coastal Louisiana, but is likely important elsewhere and is known to be important in the CSK. Based on this, we averaged and sum the fluxes data of nitrate, nitrite, and ammonium from McCarthy et al., 2015 for the GOM and Lee et al., 2012 for the CSK, respectively, and then applied $\boldsymbol{F_{Bott}^{DIN}}$ value as 1.2 mmol N m^{-2} day^{-1} in the GOM and 6.2 mmol N m^{-2} day^{-1} in the CSK. Thus, in equation 3, the benthic flux term is calculated from existing literature results after considering all DIN fluxes as above (Lee et al., 2012; McCarthy et al., 2015), and then multiplied by the area of each box.

The output terms are; 1) $\boldsymbol{F_{Export}^{DIN}}$, the exchange rate between each box in the lower layer, and 2) $\boldsymbol{F_{Deni}^{DIN}}$, the denitrification rate from the water column. Due to high stratification at the pycnocline, upward transfer of dissolved material from the lower layer to the upper layer is assumed not to occur in our model. Also, denitrification from the water column below the pycnocline is a significant N removal process, which removes up to a maximum 68% of total N input from the Mississippi River in the GOM (McCarthy et al., 2015). As the value of $\boldsymbol{F_{Deni}^{DIN}}$ in the GOM, we used a direct measurement of denitrification rates from the McCarthy et al., (2015) in the water column (88 μmol m^{-2} h^{-1}, which converted to 2.1 mmol N m^{-2} day^{-1}) where the stations were exactly same as our sub-region A, B, and C. We assumed this applied only below the pycnocline where oxygen concentrations decrease. However, in the CSK, there is no water column denitrification data because the dissolved oxygen concentration has never been down below about 4 mg L^{-1} during our data periods. Based on this, we estimated that there is a very little water column denitrification in the CSK, so we did not count this term in the CSK. Thus, we only considered the sedimentary denitrification term for the CSK region.

Water transport in the region is generally from the east, i.e., from near the Mississippi River in Sub-region A to the west, near the Atchafalaya River in Sub-region C during non-summer periods. During summer, the winds change direction from easterly to westerly, blocking the water flow to the west (Cho et al., 1998). We calculated advection from current meter data collected during the LATEX program (Nowlin et al., 1998a, b) from April 1992 to December 1994, from which we determined U (west to east flow) and V (south to north flow) components (cm s^{-1}). Figure 4 shows the mean values of coastal ocean current velocities. The annual range of the currents is 0 to 30 cm s^{-1} for the longshore component, with standard deviation of about 8 cm s^{-1}, and 0 to 7 cm s^{-1} for the cross-shelf component, with a similar standard deviation, but these current velocities are not constant and change depending on time and day. The annual current velocities in the CSK are more affected by tidal exchange and the presence of the Yellow Sea Current, but velocities are similar to those in the GOM (Jacob et al., 2000; Lim et al., 2008). The annual range of the currents is around 0 to 28 cm s^{-1} and 0 to 7 cm s^{-1} for the cross-shelf component. Thus, we used the mean value of the current velocity for the time of year during each cruise in both the GOM and the CSK for calculating the advective flow in both alongshore and onshore/offshore directions.

To run the box model, we assumed three factors: 1) the study area is in a steady state condition, with equal input sources and outputs, 2) AN-D is evenly distributed across each area, and 3) DIN is fully utilized by phytoplankton growth in the layer above the pycnocline, so we can neglect other removal factors. However, in the layer below the pycnocline, as we mentioned above, denitrification, which leads to a main loss of DIN as nitrogen gas, is considered as another output term in Equation 3. Because we assumed that all DIN removed is fully consumed by primary production above the pynocline, we can calculate potential carbon fluxes and oxygen consumption using the Redfield ratio (C: N: O: P = 106: 16: 138: 1). The PPP can be compared with ^{14}C measurement data (Lohrenz et al., 1998, 1999; Redalje et al., 1994; Quigg et al., 2011) and dissolved oxygen data from MCH mooring C at 29° N, 92° W

(4/3/2005 ~ 7/10/2005) (Bianchi et al., 2010).

Results

An N-mass balance model for the Texas-Louisiana Shelf

The existence of the three zones suggested by RC02 has been verified from winter data using nutrient/salinity relationships (Kim 2018). Figure 5 shows the contour graph based on the mean concentration of DIN at each station during the MCH M4 (March 2005) cruise. For operational and modeling purposes, stations were grouped into three sub-regions – near the Mississippi (A), near the Atchafalaya (C) and an intermediate region (B) between ~90°-91°W. During summer, it is hard to use nutrient/salinity relationships directly because riverine nutrient inputs are lower and phytoplankton growth causes rapid nutrient consumption over the shelf, leading to low overall nutrient surface concentrations. We calculated the mean [DIN] in each box, and then used the relationship between DIN and salinity to define the edges of the three zones. Near the coast salinity was consistently low, with high turbidity from the river water discharge. This was labelled the brown (river) zone.

A range of N input values from various sources were used in the N mass balance model to estimate PPP and carbon fluxes in the coastal GOM. The PPP rates were highest near the river mouth and we set the boundaries of production for each zone based on our N mass balance model results and mean [DIN] data. We defined the PPP rate of the brown zone as being over 2 gC m^{-2} day^{-1} because of the high input of N from the river, AN-D, and benthic fluxes, and the rate in the blue zone is less than 0.1 gC m^{-2} day^{-1}. The PPP rate in the green zone is then between 0.1 and 2 gC m^{-2} day^{-1}. Basically, these PPP ranges were set based on synthesized measured ranges of coastal GOM primary production, as defined for near, mid, and far fields of the coastal GOM (Dagg and Breed 2003; Lohrenz et al., 1999). Note that our model results of the PPP might overestimate the actual production because of light limitation, following RC02.

The edges of the three zones above and below the pycnocline layer, based on our N mass balance model results, are shown in Figures 6a and b. The patterns of the boundaries above and below the pycnocline differ from the edges of the zones. The brown zone was found above the pycnocline on all cruises close to the Mississippi River mouth because of the high nutrient concentrations, but only appeared off the Atchafalaya River in March 2005 (MCH M4). However, below the pycnocline it was found only in April 2004 (MCH M1) in sub-region A. This suggests that vertical transport across the pycnocline rapidly removes the high levels of suspended material that cause light limitation above the pycnocline. In the green zones, the nutrient source is mostly supported directly by the river, with minor additional sources of N from vertical sinking, AN-D, and benthic fluxes. We utilized the vertical sinking flux from the sediment trap data from Qureshi (1995) below the pycnocline layer to estimate PPP. This varied between 0.1-1.0 gN m^{-2} day^{-1} (Table 3). Typically, in the blue zone where biological production is low, vertical sinking followed by local decomposition is assumed to be the major factor that changes the nutrient concentration in the lower layer. The blue zone is always more extensive below the pycnocline than above it, which suggests there is little or no sub-pycnocline production except close to the coast and/or the river mouths, and reinforces the assumption that any chlorophyll below the pycnocline is inactive (Figure 6b). Thus, we can identify the horizontal influence of the river plume in the layer below the pycnocline and the variation in the boundaries of the three zones, based on the observed nutrient data from a bottom layer and our N mass balance model. The model suggests that regions of moderate potential productivity extend offshore at least as far as 28° 30'N in sub-region B, both above and below the pycnocline.

An N mass balance model calibration

The model calibration was done with historic literature data. Literature data suggest that observed PP rates in the green and brown zones of the coastal GOM vary between 0.4 gC m^{-2} day^{-1} (winter) and ~ 8 gC m^{-2} day^{-1} (summer) (Dagg et al., 2007; Lohrenz et al., 1998, 1999; Redalje et al., 1994). Recently, Quigg et al. (2011) measured the integrated PP rates with ^{14}C measurements during 2004 in the coastal GOM. The highest integrated PP rates were found near the Mississippi River at 3.5 gC m^{-2} day^{-1} (in July), and near the Atchafalaya River at 2.7 ~ 5.9 gC m^{-2} day^{-1} (in May to July) (in the brown and green zones). However, lowest integrated PP rates were on the outer part of the LATEX shelf (the blue zone) at 0.07 gC m^{-2} day^{-1} (in March), 0.04 ~ 0.15 gC m^{-2} day^{-1} (in May), and 0.33 ~ 0.91 gC m^{-2} day^{-1} (in July). Additionally, Quigg et al., (2011) pointed out that these higher PP values were affected by high riverine nutrients input from the MR that flows westward during that time period.

The actual PP ranges were similar with our model-based PPP (Figure 6). However, this was different from RC02's brown zone. This might be due to the differences between methods such as ^{14}C, our N-mass balance model, and RC02's theoretical model. Typically, RC02 assumed that the brown zone is light limited due to high sediment turbidity, but our model does not account for this and only considered DIN concentrations. Except for this, our PPP results are similar to direct productivity measurements from the ^{14}C incubations (Quigg et al., 2011). Our model result (PPP) showed the same range of values as ^{14}C incubations (e.g., Dagg et al., 2007; Lohrenz et al., 1998, 1999; Quigg et al., 2011; Redalje et al., 1994) in the three sub-regions.

Note that our model assumed all the biological uptake could be converted directly to production rates, which we considered as PPP. The PPP from cruises MCH M1 ~ M8 for samples from above the pycnocline calculated using our model is reasonable based on comparison with previous PP values (Figure 6a). The PPP ranges (0.01 ~ 5.05 gC m^{-2} day^{-1}) were similar to previous ^{14}C measurement PP values of between 0.04 ~ 5.9 gC m^{-2} day^{-1}.

Based on our model calculation, which assumes all the nutrients are available for production, the PPP showed maxima at all times in sub-region A (near the Mississippi river) and minima in sub-region B (between the Mississippi and Atchafalaya River), except for MCH M2 in June 2004, when sub-region C had the lowest PPP (Figure 6a). The high values in sub-region A are due largely to underutilization of nutrients in regions of high turbidity. As the water flows west under the influence of the Coriolis effect, PPP is expected to decrease as a result of declining nutrient concentrations because of dilution and nutrient uptake during biological production while the water flows to sub-region B. In sub-region C, MCH M4 (March 2005) had the highest PPP among the all MCH cruises. This probably depended on high nutrient concentrations being present during the winter period, when the region was affected by Atchafalaya River nutrient input.

Model scenarios in the Gulf of Mexico (GOM)

We tested the sensitivity of the model to changes in input/output parameters such as increasing AN-D and decreasing riverine N input. Assuming the model is robust, we investigated three model scenarios based on the nutrient distributions seen during the MCH1 cruise (note that using data from other cruises gives very similar results). In the first scenario, we cut riverine N input 60% and increased the AN-D input by a factor of two based on increasing N emission predictions (Duce et al., 2008; He et al., 2010; Kanakidou et al., 2016;

Kim (T) et al., 2011; Lawrence et al., 2000; Paerl et al., 2002). In the second scenario, we doubled the amount of AN-D as in scenario 1 and decreased riverine N input by 30% based on the hypoxia management plan goal (Gulf Hypoxia Action Plan Report, 2005, 2008; Rabalais et al. 2009). In the third scenario, we increased riverine N input by 20%, assuming the failure of the hypoxia management plan, while we set the AN-D amount equal with the first and second scenarios. Based on our N-mass balance model calculation and model scenarios, we can initially estimate carbon fluxes from our PPP rate, and, using the Redfield carbon to oxygen stoichiometry ratio (106:138), the overall oxygen balance within the coastal GOM (Table 4).

As can be seen in the scenario results for MCH M1 data (Table 4), the riverine N input source is still the major controlling factor in the coastal GOM region even when its contribution is greatly reduced and the AN-D source is doubled. For instance, if we fail to reduce riverine N input in the future (scenario 3), the potential carbon fluxes will increase by 17% relative to current conditions. In contrast, the AN-D input source only increased to a maximum of 5% of the total input term and this indicates that AN-D input is still a minor factor in the GOM. If the production is increased, overall oxygen demand will also be increased. The MCH M1 scenario result indicated that the overall oxygen demand would increase approximately 21% if we fail to reduce riverine N input, likely increasing considerably the area of the hypoxia.

An N mass balance model in the Coastal Sea off Korea (CSK)

As we have done in the GOM, we used our N mass balance model to estimate the PPP in the CSK and define the three different zones (Figure 7). Similar to the GOM region, the PPP rates were highest near the river mouth, and we set the boundaries of each zone based on our N-mass balance model results. Based on nutrient data, as was done for the GOM, we defined the brown zone as having a PPP rate above 1.5 gC m^{-2} day^{-1} because of the increased N sources from the river, AN-D, and the sediment flux. We defined the green zone as having PPP rates between 0.3 to 1.5 gC m^{-2} day^{-1} and the blue zone as having rates of less than 0.3 gC m^{-2} day^{-1}.

The seasonal results shown in Figures 7a and b show that the boundaries of the three zones above and below the pycnocline layer were roughly consistent with the main change coming in summer (August), which is the wet season and sees the highest river discharge. The large size of the green zone in all seasons suggests that AN-D is consistently adding extra nitrogen to the surface ocean along with the riverine N input. This is supported by the fact that the PPP in the blue zone is an order of magnitude higher than for the GOM. Around 90% of the grid cells in the CSK are in the same zones above and below the pycnocline (Figure 7 a and b) during all four cruises; however, in the GOM (Figure 6 a and b) this was found for fewer than half of the grid cells. This is probably due to the difference in freshwater discharge rate in the two regions, which leads to a much larger stratified area in the GOM than in the CSK.

One question that has not been investigated is the temperature dependence of primary productivity in the two areas. While the GOM is temperate throughout the year, winter temperatures in the CSK fall to ~5°C. However, according to the ocean color remote sensing images from near the CSK river mouth reported by Son et al., (2005), primary production in the CSK does not appear to be strongly affected by temperature. The PPP results of our model (0.2 to 2.2 gC m^{-2} day^{-1}) agreed with their ocean color remote sensing results (0.4 to 1.6 gC m^{-2} day^{-1}) in the CSK. Also, during all seasons, the Keum River consistently supplies high amounts of DIN (average: < 60 μM) (Lim et al., 2008) to the coastal zone (especially close to the Keum mouth). We believe, therefore, that the higher value of PPP in winter near the Keum mouth (brown zone in figure 7a), is reasonable.

The AN-D input source comes mainly from the Chinese side of the East China Sea (ECS) and this affects the boundaries of the green and blue zones above the pycnocline as it is deposited uniformly across the region. There is also nutrient input from offshore, as the Yellow Sea Bottom Cold Water Mass can up-well during the mixing process and is assumed to supply additional nutrients to the outer shelf (Lim et al., 2008).

Model scenarios in Mid-Western Coastal Sea off Korea (CSK)

AN-D is currently considerably more important (by approximately an order of magnitude) in the CSK than in the GOM), and it is anticipated that AN-D will likely be a major controlling factor here in the future (Duce et al., 2008; He et al., 2010; Kim (T) et al., 2011; Lawrence et al., 2000; Paerl et al., 2002). Because of the lack of research on potential hypoxia scenarios in Korea, we used the same three scenarios in the CSK as were used for the GOM. Similar to GOM results, riverine N input remains the major controlling factor; however, in this area, the AN-D source is more critical than in the GOM region (Table 5). The AN-D input source increased from 20% to 47% of the total input under scenario 1, while based on our scenario 3 results, increases in the AN-D input source and riverine N input together will affect biological production by increasing carbon fluxes up to 25% and oxygen demand up to 32% if we fail to reduce N input in future (Table 5).

Discussion

Most previous model studies in the GOM were focused on predicting the hypoxia area (Bierman et al., 1994; Fennel et al., 2011, 2013; Justic et al., 1996, 2002, 2003; Scavia et al., 2004). For example, Justic et al., (1996; 2003) used a two-layer model incorporating vertical oxygen data, from one station (LUMCON station C6; 28.867°N, 90.483°W), to predict the size of the hypoxia area. Similarly, Fennel et al. (2011; 2013) used her more complex simulation model, which included oxygen concentration as well as a plankton model from Fasham et al. (1990), to predict the size of the hypoxia region in the GOM. Our N mass balance model, in contrast, uses historical data from the LATEX shelf to estimate potential carbon fluxes in the GOM, and calculate the overall oxygen demand from those carbon fluxes. While this affects the total area subject to hypoxia it does not estimate the size of the hypoxic zone.

In contrast to our model, traditional predictive models have also ignored different nitrogen input sources such as AN-D and SGD. While this is probably reasonable on the Texas-Louisiana shelf, where riverine inputs dominate, it may not apply in other coastal regions. As a result, model studies in this region have concluded that reducing riverine N input is the only solution to decrease the size of the hypoxia area in the GOM (Gulf Hypoxia Action Plan Report, 2005, 2008; Rabalais et al. 2009; Scavia et al., 2013). According to our model results, AN-D is still a minor controlling factor in the GOM; however, in the CSK, the AN-D contributed more to the total nitrogen budget and may be a major controlling factor in the future. This indicates that AN-D should be considered as another input term for nutrient managements, especially in Asia or in other regions where high concentrations are expected. Similarly, nitrogen input from either sediment fluxes or groundwater also need to be considered.

Our zonal boundaries can be compared with the results of Lahiry (2007), who used salinity to define the edges of each zone for the three cruises MCH M1, M2, and M3 (Figure 8) and defined the edges of the RC02 zones in the coastal GOM based solely on salinity. Her limited simulation results indicated similar patterns to our model based on DIN concentration near the Mississippi River mouth (e.g., during MCH M1, M2, and M3). Mixing was more conservative in this region than further west because the low salinity water with high nutrients was less diluted with offshore water.

Away from the MR in sub-regions B and C, however, her results gave very different boundaries for the three zones compared with our results (Figure 8). In particular, the results near the Atchafalaya River were very different (compare Figures 6 and 8). For example, our data showed only green and blue zones off Atchafalaya Bay during MCH M1, with no brown zone. Similarly, the extent of the blue zones in sub-region C during MCH M2 and M3 is also very different. We believe that our DIN-model based classification can cover more complex biological processes than the Lahiry (2007) method, which considers only advection and mixing and the DIN-model is a more sensible way to look at biological processes in the GOM.

Our results also agree with previous studies that demonstrated that both the GOM and CSK regions are N-limited for most of the year (Kim (G) et al., 2011; Turner and Rabalais, 2013). This compares with the results of Sylvan et al., (2007), who reported that the coastal GOM could be P-limited in the MR delta mouth area where our brown zone is located, while RC02 suggested light-limitation rather than N- or P-limitation. However, this P-limited condition appears to occur when N concentrations are very high. In particular, the N/P ratios in the both the GOM and CSK during our sampling were less than 16, indicating that both regions were N-limited, although a few stations in the brown zone near the MR river area had ratios of between 16 and 18 (Figure 9). These higher N/P ratios may result from the high sediment turbidity causing light-limited conditions in this zone near the river mouth (Rowe and Chapman, 2002).

It should be remembered, however, that the arithmetic N:P value per se is unimportant in determining nutrient limitation. As long as both nutrients can be measured, it is theoretically possible for phytoplankton to continue to grow. The MARS has generally such an excess of N relative to P that N:P ratios >>16 can be expected as P concentrations fall, but this does not necessarily mean that productivity is limited, and we never found P concentrations of zero in any of our sub-regions; the lowest P concentration measured during all cruises in the GOM and CSK was 0.2 μM.

Both the GOM and CSK regions receive nitrogen inputs from AN-D, rivers, and benthic fluxes. These different nitrogen input sources control coastal productivity, and this may reflect the different nitrogen cycling in the two regions. In the GOM, the riverine N input source consistently dominates coastal productivity and eutrophication, while, in the CSK, AN-D is also becoming a critical controlling factor. In the CSK, however, there is strong tidal mixing of freshwater from the Keum River and/or Gyunggi Bay with nearby coastal water, which results in a tidal front along the offshore region and off the Taean Peninsula during spring and summer. It is this physical mixing that mostly controls the spatial distribution patterns of nutrients and salinity here, particularly below the pycnocline (Lim et al., 2008). The brown zone in the upper layer in the CSK (August 2008) changed to a green zone region below the pycnocline layer as a result of the strong coastal tidal mixing.

RC02 considered their model to be theoretical. In the brown zone, close to the river mouth, they assumed turbidity leads to light-limited conditions. Their results agree well with measured ^{14}C PP numbers from Quigg et al. (2011) who found the lowest integrated PP is near the MR delta mouth. However, our N mass balance model did not consider light limitation and therefore PPP in the brown zone is high. Such good agreement suggests that our model can be applied to a wide region, while ^{14}C measurements are typically conducted at a few specific points, as long as such limitations are taken into account.

In the CSK, most previous production studies focused on inshore areas such as estuaries or rivers. Our research focused for the first time on the coastal ocean off Korea. Our results explained that diverse nitrogen sources need to be recognized as potential issues for future nutrient management concerned with hypoxia, eutrophication, or other environmental issues. The agreement between our results and the pattern of production based on satellite-sensing in the CSK (Son et al., 2005), suggests that our model is reasonable.

The results of our changing scenarios represent how the biological processes in these coastal regions may vary as individual nutrient sources change; in the near future both AN-D flux and riverine N flux need to be considered for managing nitrogen in coastal waters. While our model cannot predict the area of the hypoxic zone, we can investigate the effects of potential flux changes of each factor, such as AN-D, riverine input, or benthic fluxes, and calculate the effects of changes in each on PPP and on the overall oxygen balance for the region. We have only considered different input terms of our N mass balance model; output terms such as water mixing rates and the residence time for each box need more detailed study in future work to calculate more realistic production changes in each box.

Conclusion

The model suggests that the three zone theory of RC02 can be applied not only in the northern GOM but also in the CSK region and that three zones can be distinguished based on their nutrient concentration. As a result, we believe that using our N mass balance model to separate different zones based on RC02 may be appropriate not only for large-scale regions like the GOM and CSK but also at small scales such as river or estuary systems. The model also estimates potential primary production and carbon flux based on the inclusion of AN-D data that have not been considered previously (e.g. Bierman et al., 1994; Kim (T) et al., 2011). Our results agree well with previous ^{14}C measurements in the GOM (Quigg et al., 2011) and ocean color remote sensing in the CSK (Son et al., 2005).

Based on CSK cruise data results, we can initially determine where the three different zones are in the CSK. We identified the brown zone close to the Keum River mouth and the green and blue zones further away from the coast of Korea.

We evaluated our model and tested its sensitivity based on three different scenarios. Through our scenario results, we assume that the AN-D is a considerable factor in the CSK as well as the riverine N input from the Keum river. Reducing nutrient input from the river is critical for hypoxia management policy (Gulf Hypoxia Action Plan Report, 2005, 2008; Rabalais et al. 2009). In addition, these model scenarios will be helpful in future coastal nutrient management or hypoxia management studies in the CSK, especially as AN-D sources become more important.

Acknowledgements

The authors would like to thank to the captain and crew of the R/V Gyre along with the marine technicians and students who participated in the cruises. This project was funded by NOAA Center for Sponsored Coastal Ocean Research, Grant Numbers: NA03NOS4780039, NA06NOS4780198, and NA09NOS4780208.

References

Anderson, G. C.: Subsurface chlorophyll maximum in the northeast Pacific Ocean. Limnology and Oceanography., 14(3), 386-391, 1969.

Alexander, R. B., Smith, R. A., Schwartz, G. E., Preston, S. D., Brakebill, J. W., Srinivasan, R., and Pacheco, A. P.: Atmospheric nitrogen flux from the watersheds of major estuaries of the United States: An application of the SPARROW watershed model., 119-170, 2000.

Alexander, R. B., Smith, R. A., Schwarz, G. E., Boyer, E. W., Nolan, J. V., and Brakebill, J. W.: Differences in phosphorus and nitrogen delivery to the Gulf of Mexico from the Mississippi river basin. Environmental Science and Technology., 42, 822-830, 2008.

Belabbassi, L.: Examination of the relationship of river water to occurrences of bottom water with reduced oxygen concentrations in the northern Gulf of Mexico. Texas A & M University. Ph.D. Dissertation., 2006.

Bianchi, T. S., DiMarco, S. F., Cowan, Jr. JH., Hetland, R. D., Chapman, P., Day, J. W., and Allison, M. A.: The Science of hypoxia in the Northern Gulf of Mexico: A review. Science of the total Environment., 408(7), 1471-1484, 2010.

Bierman, V. J., Hinz, S. C., Wiseman, Jr. W. J., Rabalais, N. N., and Turner, R. E.: A Preliminary Mass Balance Model of Primary Productivity and Dissolved Oxygen in the Mississippi River Plume/Inner Gulf Shelf Region. Estuaries., 17(4), 886-899, 1994.

Bode, A., and Dortch, Q.: Uptake and regeneration of inorganic nitrogen in coastal waters influenced by the Mississippi River: spatial and seasonal variations. Journal of Plankton Resources., 18, 2251-2268, 1996.

Castro, M. S., Driscoll, C. T., Jordan, T. W., Reay, W. G., Boynton, W. R., Seitzinger, S. P., Styles, R. V., and Cable, J. E.: Contribution of atmospheric deposition to the total nitrogen loads to thirty-four estuaries on the Atlantic and Gulf coasts of the United States, 77–106, 2000.

Castro, M. S., and Driscoll, C. T.: Atmospheric nitrogen deposition to estuaries in the mid-Atlantic and northeastern United States. Environmental science & technology., 36(15), 3242-9, 2002.

Cho, K. R., Reid, O., and Nowlin, Jr W. D.: Objectively mapped stream function fields on the Texas-Louisana shelf based on 32 months of moored current meter data. Journal of Geophysics Research., 103(C5), 10377-10390, 1998.

Choi, H. Y., Lee, S. H., and Oh, I. S.: Quantitative Analysis of the Thermal Front in the Mid-Eastern Coastal Area of the Yellow Sea. Journal of the Korean Society of Oceanography [The Sea]., 3, 1-8, 1998.

Choi, H. Y., Lee, S. H., and Yoo, K. Y.: Salinity Distribution in the Mid-eastern Yellow Sea during the High Discharge from the Keum River Weir. Journal of the Korean Society of Oceanography [The Sea]., 4, 1-9, 1999.

Christensen, P. B., Rysgaard, S., Sloth, N. P., Dalsgaard, T., and Schwaerter, S.: Sediment mineralization, nutrient fluxes, denitrification and dissimilatory nitrate reduction to ammonium in an estuarine fjord with sea cage trout farms. Aquatic Microbial Ecology., 21, 73-84, 2000.

Cornell, S., Rendell, A., and Jickells, T.: Atmospheric inputs of dissolved organic nitrogen to the oceans. Nature., 376, 243-246, 1995.

Dagg, M. J., and Breed, G. A.: Biological effects of Mississippi River nitrogen on the northern Gulf of Mexico-a review and synthesis. Journal of Marine Systems., 43, 133-152, 2003.

Dagg, M. J., Ammerman, J. W., AMON, R. M. W., Gardner, W. S., Green, R. E., Lohrenz, S. E.: A review of water column processes influencing hypoxia in the northern Gulf of Mexico. Estuaries Coasts., 30, 735-752, 2007.

Dalsgaard, T.: Benthic primary production and nutrient cycling in sediments with benthic microalgae and transient accumulation of macroalgae. Limnology and Oceanography., 48(6), 2138-2150, 2003.

De Boer, A. M., Watson, A. J., Edwards, N. R., and Oliver, K. I. C.: A multi-variable box model approach to the soft tissue carbon pump. Climate of the past., 6, 827-841, 2010.

Diaz, R. J., and Rosenberg, R.: Marine benthic hypoxia: A review of its ecological effects and the behavioural responses of benthic macrofauna. Oceanography Marine Biology. Ann. Rev., 33, 245-303, 1995.

Diaz, R. J., and Rosenberg, R.: Spreading dead zones and consequences for marine ecosystems. Science., 321(5891), 926-9, 2008.

DiMarco, S. F., and Zimmerle, H. M.: MCH Atlas: Oceanographic Observations of the Mechanisms Controlling Hypoxia Project. Texas A&M University, Texas Sea Grant, College Station, TX. Publication TAMU-SG- 17-601,350. ISBN 978-0-692-87961-0, 2017.

Dodds, W. K., and Smith, V. H.: Nitrogen, phosphorus, and eutrophication in streams. Inland Waters., 6, 155-164, 2016.

Doney, S. C., Mahowald, N., Lima, L., Feely, R. A., Mackenzie, F. T., Lamarque, J. F., and Rasch, P. J.: Impact of anthropogenic atmospheric nitrogen and sulfur deposition on ocean acidification and the inorganic carbon system. Proceedings of the National Academy of Science., 104, 14580-14585, 2007.

Dortch, Q., and Whitledge, T. E.: Does nitrogen or silicon limit phytoplankton in the Mississippi River plume and nearby regions? Continental Shelf Research., 12, 1293-1309, 1992.

Duce, R. A., LaRoche, J., Altierl, K., Arrigo, K. R., Baker, A. R., Capone, D. G., Cornell, S., Dentener, F., Galloway, J., Ganeshram, R. S., Geider, R. J., Jickells, T., Kuypers, M. M., Langlois, R., Liss, P. S., Liu, S. M., Middelburg, J. J., Moore, C. M., Nickovic, S., Oschlies, A., Pedersen, T., Prospero, J., Schlitzer, R., Seitzinger, S., Sorensen, L. L., Uematsu, M., Ulloa, O., Voss, M., Ward, B., and Zamora, L.: Impacts of Atmospheric Anthropogenic Nitrogen on the Open Ocean. Science., 320, 893-897, 2008.

Fasham, M. J. R., Ducklow, H. W., and Mckelvie, S. M.: A nitrogen-based model of plankton dynamics in the oceanic mixed layer. Journal of Marine research., 48 ,591-639, 1990.

Feng, Y., DiMarco, S. F., and Jackson, G. A.: Relative role of wind forcing and riverine nutrient input on the extent of hypoxia in the northern Gulf of Mexico. Geophysical Research Letters., 39, L09601, 2012.

Feng, Y., Fennel, K., Jackson, G. A., DiMarco, S. F., and Hetland, R. D.: A model study of the response of hypoxia to upwelling-favorable wind on the northern Gulf of Mexico shelf. Journal of Marine Systems., 131, 63-73, 2014.

Fennel, K., Wilkin, J., Levin, J., Moisan, J., O’Reilly, J., and Haidvogel, D.: Nitrogen cycling in the Middle Atlantic Bight: Results from a three-dimensional model and implications for the North Atlantic nitrogen budget. Global Biogeochemical cycles., 20, GB3007, doi:10.1029/2005G, 2006.

Fennel, K., Hetland, R. D., Feng, Y., and DiMarco, S. F.: A coupled physical-biological model of the Northern Gulf of Mexico shelf: model description, validation and analysis of phytoplankton variability. Biogeosciences., 8, 1881-1899, 2011.

Fennel, K., Hu, J., Laurent, A., Marta-Almeida, M., and Hetland, D. R.: Sensitivity of hypoxia predictions for the northern Gulf of Mexico to sediment oxygen consumption and model nesting. Journal of Geophysical Research: Oceans., 118, 990-1002, 2013.

Forrest, D. R., Hetlandl R. D., and DiMarco, S. F.: Multivariable statistical regression models of the areal extent of hypoxia over the Texas–Louisiana continental shelf. Environmental Research Letters., 6, 045002, 2011.

Goolsby, D. A. Mississippi basin nitrogen flux believed to cause Gulf hypoxia., EOS Transactions 2000:29–321, 2000.

Green, R. E., Gould, Jr. R. W., and Ko, D. S.: Statistical models for sediment/detritus and dissolved absorption coefficients in coastal waters of the northern Gulf of Mexico. Continental Shelf Research., 28(10), 1273-1285, 2008.

Gulf Hypoxia Action Plan Report. Mississippi River Gulf of Mexico Watershed Nutrient Task Force., 2005.

Gulf Hypoxia Action Plan Report. Mississippi River Gulf of Mexico Watershed Nutrient Task Force., 2008.

Hagy, J. D., Sanford, L. P., and Boynton. W. R.: Estimation of net physical transport and hydraulic residence times for a coastal plain estuary using box models., Estuaries 23:328–340. doi:10.2307/1353325, 2000.

He, C. H., Wang, X., Liu, X., Fangmeler, A., Christie, P., and Zhang, F.: Nitrogen deposition and its contribution to nutrient inputs to intensively managed agricultural ecosystems. Ecological Application., 20(1), 80-90, 2010.

Hetland, R. D., and DiMarco, S. F.: How does the character of oxygen demand control the structure of hypoxia on the Texas-Louisiana continental shelf? Journal of Marine Systems., 70, 49-62, 2008.

Howarth, R. W., and Marino, R.: Nitrogen as the limiting nutrient for eutrophication in coastal marine ecosystems: Evolving views over three decades. Limnology and Oceanography., 51(1), 364-376, 2006.

Jacob, G. A., Hur, H. B., and Riedlinger, S. K.: Yellow and East China Seas response to winds and currents. Journals of Geophysical Research., 105 (21), 947-968, 2000.

Justic, D., Rabalais, N. N., and Turner, R. E.: Effects of climate change on hypoxia in coastal waters; A doubled CO2 scenario for the northern Gulf of Mexico. Limnology and Oceanography., 41(5), 992-1003, 1996.

Justic, D., Rabalais, N. N., and Turner, R. E.: Modeling the impacts of decadal changes in riverine nutrient fluxes on coastal eutrophication near the Mississippi River Delta. Ecological Modelling., 152, 33-46, 2002.

Justic, D., Rabalais, N. N., and Turner, R. E.: Simulated responses of the Gulf of Mexico hypoxia to variations in climate and anthropogenic nutrient loading. Journal of Marine Systems., 42, 115-126, 2003.

Kanakidou, M., Myriokefalitakis, S., Daskalakis, N., and Fanourgakis, G.: Past, Present, and Future Atmospheric Nitrogen Deposition. American Meteorological Society., 73(5), 2039-2047, 2016.

Kim, G., Kim, J. S., and Hwang, D. W.: Submarine groundwater discharge from oceanic islands standing in oligotrophic oceans: Implications for global production and organic carbon fluxes. Limnology and Oceanography., 56(2), 673-682, 2011.

Kim, J. S., Lee, M. J., Kim, J., and Kim, G.: Measurement of Temporal and Horizontal Variations in 222Rn Activity in Estuarine Waters for Tracing Groundwater Inputs. Ocean Science Journal., 45(4), 197-202, 2010.

Kim, J. S.: Implications of different nitrogen input sources for primary production and carbon flux estimates in coastal waters. Texas A&M University. Ph.D. Dissertation., 2018.

Kim, J. Y., Ghim, Y. S., Lee, S. B., Moon, K. C., Shim, S. G., Bae, G. N., and Yoon, S. C.: Atmospheric Deposition of Nitrogen and Sulfur in the Yellow Sea Region: Significance of Long-Range Transport in East Asia. Water, Air, and Soil Pollution., 205, 259-272, 2010.

Kim, T. W., Lee, K., Najjar, R. G., Jeong, H. D., and Jeong, H. J.: Increasing N abundance in the northwestern Pacific Ocean due to atmospheric nitrogen deposition. Science., 334, 505-509, 2011.

Lahiry, S.: Relationships between nutrients and dissolved oxygen concentrations on the Texas-Louisiana shelf during spring-summer of 2004. Texas A & M University. MS. Thesis., 2007.

Lamarque, J. F., Dentener, F., McConnell. J., Ro. C. U., Shaw. M., Vet. R., Bergmann. D., Cameron-Smith. P., Dalsoren. S., Doherty. R., Faluvegi. G., Ghan. S. J., Josse. B., Lee. Y. H., MacKenzie. I. A., Plummer. D., Shindell. D. T., Skeie. R. B., Stevenson. D. S., Strode. S., Zeng. G., Curran. M., Dahl-Jensen. D., Das. S., Fritzsche. D., and Nolan. M.: Multi-model mean nitrogen and sulfur deposition from the Atmospheric Chemistry and Climate Model Intercomparison Project (ACCMIP): evaluation of historical and projected future changes. Atmospheric Chemistry and Physics., 13, 7997-8018, 2013.

Lawrence, G. B., Goolsby, D. A., Battaglin, W. A., and Stensland, G. J.: Atmospheric nitrogen in the Mississippi River Basin-emissions, deposition and transport. Science of The Total Environment., 248(2-3), 87-100, 2000.

Laurent, A., Fennel, K., Hu, J., and Hetland, R. D.: Simulating the effects of phosphorus limitation in the Mississippi and Atchafalaya River plumes. Biogeosciences., 9, 4797-4723, 2012.

Lee, J. S., Kim, K. H., Shim, J. H., Han, J. H., Choi, Y. H., and Khang, B. J.: Massive sedimentation of fine sediment with organic matter and enhanced benthic-pelagic coupling by an artificial dyke in semi-enclosed Chonsu Bay, Korea. Marine Pollution Bulletin., 64, 153-163, 2012.

Lim, D., Kang, M. R., Jang, P. G., Kim, S. Y., Jung, H. S., Kang, Y. S., and Kang, U. S.: Water Quality Characteristics Along Mid-Western Coastal Area of Korea. Ocean and Polar Research., 30(4), 379-399, 2008.

Liu, S. M., Zhang, J., Chen, S. Z., Chen, H. T., Hong, G. H., Wei, H., and Wu, Q. M.: Inventory of nutrient compounds in the Yellow Sea. Continental Shelf Research., 23, 1161-1174, 2003.

Lehrter, J. C., Beddick Jr., D. L., Devereux, R., Yates, D. F., and Murrell. M. C.: Sediment-water fluxes of dissolved inorganic carbon, O2, nutrients, and N_2 from the hypoxic region of the Louisiana continental shelf. Biogeochemistry, 109, 233–252, 2012.

Lohrenz, S. E., Wiesenburg, D. A., Arnone, R. A., and Chen, X. G.: What controls primary production in the Gulf of Mexico? In: Sherman K, Kumpf H, Steidinger K (ed) The Gulf of Mexico Large Marine Ecosystem: Assessment, sustainability and management. Blackwell Science, Malden, MA., 151-170, 1998.

Lohrenz, S. E., Fahnenstiel, G. L., Redalje, D. G., Lang, G. A., Dagg, M. J., Whitledge, T. E., and Dortch, Q.: Nutrients, irradiance, and mixing as factors regulating primary production in coastal waters impacted by the Mississippi River plume. Continental Shelf Research., 19, 1113-1141, 1999.

Luo, X. S., Tang, A. H., Shi, K., Wu, L. H., Li, W. Q., Shi, W. Q., Shi, X. K., Erisman, J. W., Zhang, F. S., and Liu, X. J.: Chinese coastal seas are facing heavy atmospheric nitrogen deposition. Environmental Research Letters., 9, 1-10, 2014.

McCarthy, M. J., Newell, S. E., Carini, S. A., and Cardner, W. S.: Denitrification dominates sediment nitrogen removal and is enhanced by bottom-water hypoxia in the Northern Gulf of Mexico. Estuaries and Coasts., 38, 2279-2294. 2015.

Milliman, J. D., and Meade, R. H.: World-wide delivery of river sediment to the oceans. The Journal of Geology., 91(1), 1-21, 1983.

Nipper, M., Sanchez Chavez, J. A., Tunnell, Jr. J. W.: “Marsh Island,” “Calcasieu Lake,” and “General Facts about the Gulf of Mexico.” GulfBase: Resource Database for Gulf of Mexico Research., 2004.

Nowlin, W. D. Jr., Jochens, A. E., Reid, R. O., and DiMarco, S. F.: Texas-Louisiana Shelf Circulation and Transport processes Study: Synthesis Report, Volume I: Technical Report. OCS Study MMS 98-0035. U.S. Dept. of the Interior, Minerals Mgmt Service, Gulf of Mexico OCS Region, New Orleans, LA., 502, 1998a.

Nowlin, W. D. Jr., Jochens, A. E., Reid, R. O., and DiMarco, S. F.: Texas-Louisiana Shelf Circulation and Transport processes Study: Synthesis Report, Volume II: Appendices. OCS Study MMS 98-0036. U.S. Dept. of the Interior, Minerals Mgmt Service, Gulf of Mexico OCS Region, New Orleans, LA., 288, 1998b.

Nunnally, C., Quigg, A., DiMarco, S. F., Chapman, P., and Rowe, G. T.: Benthic-Pelagic Coupling in the Gulf of Mexico Hypoxic Area: Sedimentary enhancement of hypoxic conditions and near bottom primary production. Continental Shelf Research., 85, 143-152, 2014.

Paerl, H. W., Dennis, R. L., and Whitall, D. R.: Atmospheric Deposition of Nitrogen: Implications for Nutrient Over-Enrichment of Coastal Waters. Estuaries., 25(4B), 677-693, 2002.

Paerl, H. W.: Controlling Eutrophication along the Freshwater-Marine Continuum: Dual Nutrient (N and P) Reductions are Essential. Estuaries and Coasts., 32, 593-601, 2009.

Park, M. J., Savenije, H. H. G., Cai, H., Jee, E. K., and Kim, N. H.: Progressive change of tidal wave characteristics from the eastern Yellow Sea to the Asan Bay, a strongly convergent bay in the west coast of Korea. Ocean Dynamics., 67, 1137-1150, 2017.

Park, Y. H.: Analysis of characteristics of Dynamic Tidal Power on the west coast of Korea. Renewable and Sustainable Energy Reviews., 68, 461-474, 2017.

Qureshi, N. A.: The role of fecal pellets in the flux of carbon to the sea floor on a river-influenced continental shelf subject to hypoxia. Louisiana State University. Ph.D. Dissertation., 1995.

Quigg, A., Sylvan, J., Gustafson, A., Fisher, T., Oliver, R., Tozzi, S., and Ammerman, J.: Going west: nutrient limitation of primary production in the northern Gulf of Mexico and the importance of the Atchafalaya River. Aquatic Geochemistry., 17, 519-544, 2011.

Rabalais, N. N., and Smith, L. E.: The effects of bottom water hypoxia on benthic communities of the southeastern Louisiana continental shelf. New Orleans, Louisiana, U.S. Minerals Management Service, Gulf of Mexico OCS Region.,105, 1995.

Rabalais, N. N., and Turner, R. E.: Hypoxia in the Northern Gulf of Mexico: Description, causes and change, pp. 1–36. In N. N. Rabalais and R. E. Turner (eds.), Coastal Hypoxia: Consequences for Living Resources and Ecosystems. Coastal and Estuarine Studies., 58, 2001.

Rabalais, N. N., Turner, R. E., and Scavia, D.: Beyond science into policy: Gulf of Mexico hypoxia and the Mississippi river. Bioscience. Vol.52(2). pp.129-142, 2002.

Rabalais, N. N., Turner, R. E., Sen Gupta, B. K., Boesch, D. F., Chapman, P., and Murrell, M. C.: Hypoxia in the northern Gulf of Mexico: Does the science support the plan to reduce, mitigate, and control hypoxia? Estuaries Coastal., 30, 753-772, 2007.

Rabalais, N. N., Turner, R. E., Justic, D., Diaz, R. J.: Global change and eutrophication of coastal waters. ICES. Journal of Marine Science., 66, 1528–1537, 2009.

Ramesh. R., Chen. Z., Cummins. V., Day. J., D'Elia. C., Dennison. B., Forbes. D. L., Glaeser. B., Claser. M., Clavovic. B., Kremer. H., Lange. M., Larsen. J. N., Tissier. M. Le., Newton.

A., Pelling. M., Purvaja. R., and Wolanski. E.: Land-ocean interactions in the coastal zone: past, present & future, Anthtropocene., 12, 85-98, 2015.

Redalje, D. G., Lohrenz, S. E., and Fahnenstiel, G. L.: The relationship between primary production and the vertical export of particulate organic matter in a river impacted coastal ecosystem. Estuaries., 17, 829-838, 1994.

Robertson, D. M., and Saad, D. A.: SPARROW Models Used to Understand Nutrient Sources in the Mississippi/Atchafalaya River Basin. Journal of Environmental Quality., 42, 1422-1440, 2014.

Rowe, G. T., and Chapman, P.: Continental Shelf Hypoxia: some nagging questions. Gulf Mexico Science., 20, 153-160, 2002.

Rowe, G. T., Kaegi, M. E. C., Morse, J. W., Boland, G. S., and Briones, E. G. E.: Sediment community metabolism associated with continental shelf hypoxia, northern Gulf of Mexico. Estuaries., 25(6), 1097–1106, 2002.

Scavia, D., Justic, D., and Bierman, V. J.: Reducing Hypoxia in the Gulf of Mexico: Advice from Three Models. Estuaries., 27(3), 419-425. 2004.

Scavia, D., Evans, M. A., and Obenour, D. R.: A scenario and forecast model for Gulf of Mexico hypoxic area and volume. Environmental Science and Technology., 47, 10423-10428, 2013.

Shou, W., Zong, H., Ding, P., and Hou, L.: A modelling approach to assess the effects of atmospheric nitrogen deposition on the marine ecosystem in the Bohai Sea, China. Esruarine, Coastal and Shelf Science., 208, 36-48, 2018.

Sigman, D. M., and Hain, M. P.: The Biological Productivity of the Ocean. Nature Education., 3, 1-16, 2012.

Son, S. H., Campbell, J. W., Dowell, M., Yoo, S. J., and Noh, J.: Primary production in the Yellow Sea determined by ocean color remote sensing. Marine Ecology Progress Series., 303, 91-103, 2005.

Sylvan, J. B., Dortch, Q., Nelson, D. M., Maier Brown, A. F., Morrison, W., Ammerman, J. W.: Phosphorus limits phytoplankton growth on the Louisiana shelf during the period of hypoxia formation. Environmental Science and Technology., 40(24), 7548– 7553, 2006.

Testa, J. M., Kemp. W. M., Boynton. W. R., and Hagy. J. D: Long-term changes in water quality and productivity in the Patuxent river estuary: 1985 to 2003. Estuaries and Coasts., 31, 1021-1037, 2008.

Thornton, D. C. O., Dong, L. F., Underwood, G. J. C., and Nedwell, D. B.: Sediment-water inorganic nutrient exchange and nitrogen budgets in the Colne Estuary, UK. Marine Ecology Progress Series., 337, 63-77, 2007.

Turner, R. E., and Rabalais, N. N.: Changes in the Mississippi River nutrient supply and offshore silicate-based phytoplankton community responses. In Dyer, K.R and R. J Orth(eds.). Changes in Fluxes in Estuaries: Implications from Science to management Proceedings of ECSA22/ERF Symposium. International Symposium Series. Olsen and Olsen. Gredensborg. Denmark.,147-150, 1994.

Turner, R. E., Rabalais, N. N., and Justic, D.: Predicting summer hypoxia in the northern Gulf of Mexico: riverine N, P and Si loading. Marine Pollution Bulletin., 51, 139-148, 2006.

Turner, R. E., Rabalais, N. N., and Justic, D.: Gulf of Mexico Hypoxia: Alternate States and a Legacy. Environmental Science and Technol., 42, 2323-2327, 2008.

Turner, R. E., and Rabalais, N. N.: Nitrogen and phosphorus phytoplankton growth limitation in the northern Gulf of Mexico. Aquatic microbial ecology., 68, 159–169, 2013.

Wade, T. L., and Sweet, S. T.: Final Report Coastal Bend Bays and Estuaries Program (CBBEP): Atmospheric Deposition Study., 48pp, 2008.

Wang, H., Dai, M., Liu, J., Kao, S. J., Zhang, C., Cai, W. J., Wang, G., Qian, W., Zhao, M., and Sun, Z.: Eutrophication-Driven Hypoxia in the East China Sea off the Changjiang Estuary. Environmental Science & Technology., 50, 2255-2263, 2016.

Yang, J. S., and Ahn, T. Y.: The analysis of the correlation between groundwater level and the moving average of precipitation in Kuem river watershed. The Journal of Engineering Geology., 18, 1-6, 2008.

Zhao, Y., Zhang, L., Pan, Y., Wang, Y., Paulot, F., and Henze, D. K.: Atmospheric nitrogen deposition to the northwestern Pacific: seasonal variation and source attribution. Atmos. Chem. Phys., 15, 10905-10924, 2015.

List of Figures

Figure 1. Study sites and sampling areas in the GOM and Korea. Figure (a) shows the sampling area within the northern GOM, and (b) shows station positions from March 2005. Note that MCH project data are widely distributed across the region. Figure (c) shows the sampling area off the west coast of Korea and (d) shows all of the station positions.

Figure 2. The Rowe and Chapman three zone hypothesis, which described the physical and biochemical processes that initiate and sustain hypoxia on the Texas-Louisiana Shelf, [Rowe and Chapman, 2002]. *Reprinted with permission of Gulf of Mexico Science.*

Figure 3. (a) Input (blue) and output (red) sources for each 0.25° box in the GOM and CSK (see text for details); (b) Area of each sub-region (red) and boxes affected by direct riverine input (blue) in the GOM. Export N (Mixing) represents the advective transport term. The processes of biogeochemical and transport processes of both regions are the same and each in/out put factor is the same in the GOM and CSK. Note that transfer between boxes occurs in both directions alongshore and onshore/offshore and is not a one-dimensional process as suggested in the diagram.

Figure 4. Mean ocean current velocities (a) and standard deviations (b) for biweekly periods from August 1993 through December 1994 based on data from LATEX project. Positive values of U show eastward flow; positive values of V show northward flow.

Figure 5. Extent of the three zones defined by RC02 based on the mean concentration of nutrient (DIN) at each station during the MCH M4 cruise in March 2005, showing their correspondence to the three sub-regions used in the box model. Red, grey and blue stations correspond to sub-regions A (near the Mississippi River), B (between the Mississippi and Atchafalaya), and C (near the Atchafalaya) respectively.

Figure 6a. Areal distributions of the three zones using data from above the pycnocline, based on N mass balance model results. Colors and numbers represent boxes found in each of the three zones in terms of potential productivity (Unit: gC m^{-2} day^{-1}).

Figure 6b. As for 6a, using data from below the pycnocline.

Figure 7a. The distribution of the three zones off Mid-western Korea (CSK) above the pycnocline based on the RC02 hypothesis applied to the N mass balance model. Colors and numbers represent boxes found in each of the three zones in terms of potential productivity (Unit: gC m^{-2} day^{-1}).

Figure 7b. As for 7a, using data from below the pycnocline

Figure 8. Distribution of the three zones during cruises MCH M1-M3 based on salinity data (Lahiry, 2007). Areas shaded in three colors represent the brown, green and blue zones respectively.

Figure 9. DIN against DIP during sampling periods in the GOM and CSK. Nearly all samples

had an N:P ratio of < 16, which indicated potential N-limited condition. At a few points near the brown zone the ratio was between 16 -18; this is where light-limitation is expected according to RC02.

List of Tables

Table 1. Sampling dates for data from Gulf of Mexico projects and the coastal sea of Korea. Winter data are listed for the Gulf of Mexico cruises.

Table 2. Atmospheric Nitrogen Deposition (AN-D) in the USA and in the Yellow Sea.

Table 3. Definitions and values used in N-mass balance model to calculate DIN removal by biological production. (a) Each one quarter degree box; (b) Wade and Sweet 2008 for GOM region; (c) McCarthy et al., 2015 (d) Lee et al., 2012; (e) McCarthy et al., 2015; (f) Qureshi 1995. *$\boldsymbol{F_{Atmo}^{DIN}}$ of CSK region is used as mean values of Asia data in Table 2, which is initially 5 times higher than that of GOM (1.4 X 10^5 mol day^{-1}). ** The unit of $\boldsymbol{F_{Sink}^{DIN}}$ was converted to mol day^{-1} from the unit of original data (gN m^{-2} day^{-1}) with area of box (0.25 m x 0.25 m) and molar mass of N (14 g mol $^{-1}$). All unit were converted to mol day^{-1} multiplied by area of box (0.25 m x 0.25 m).

Table 4. Simulation results for selected model scenarios based on MCH M1 (April 5-7, 2004), as described in the text. Biological production is calculated using our N-mass balance model, while oxygen demand is calculated by the Redfield stoichiometry ratio (C: O_2 = 106: 138) (Unit: gC m^{-2} day^{-1}).

Table 5. Simulation results for selected model scenarios based on CSK (February 2008) data, as described in the text. Biological production is calculated using our N-mass balance model, while oxygen demand is calculated by the Redfield stoichiometry ratio (C: O_2 = 106: 138) (Unit: gC m^{-2} day^{-1}).

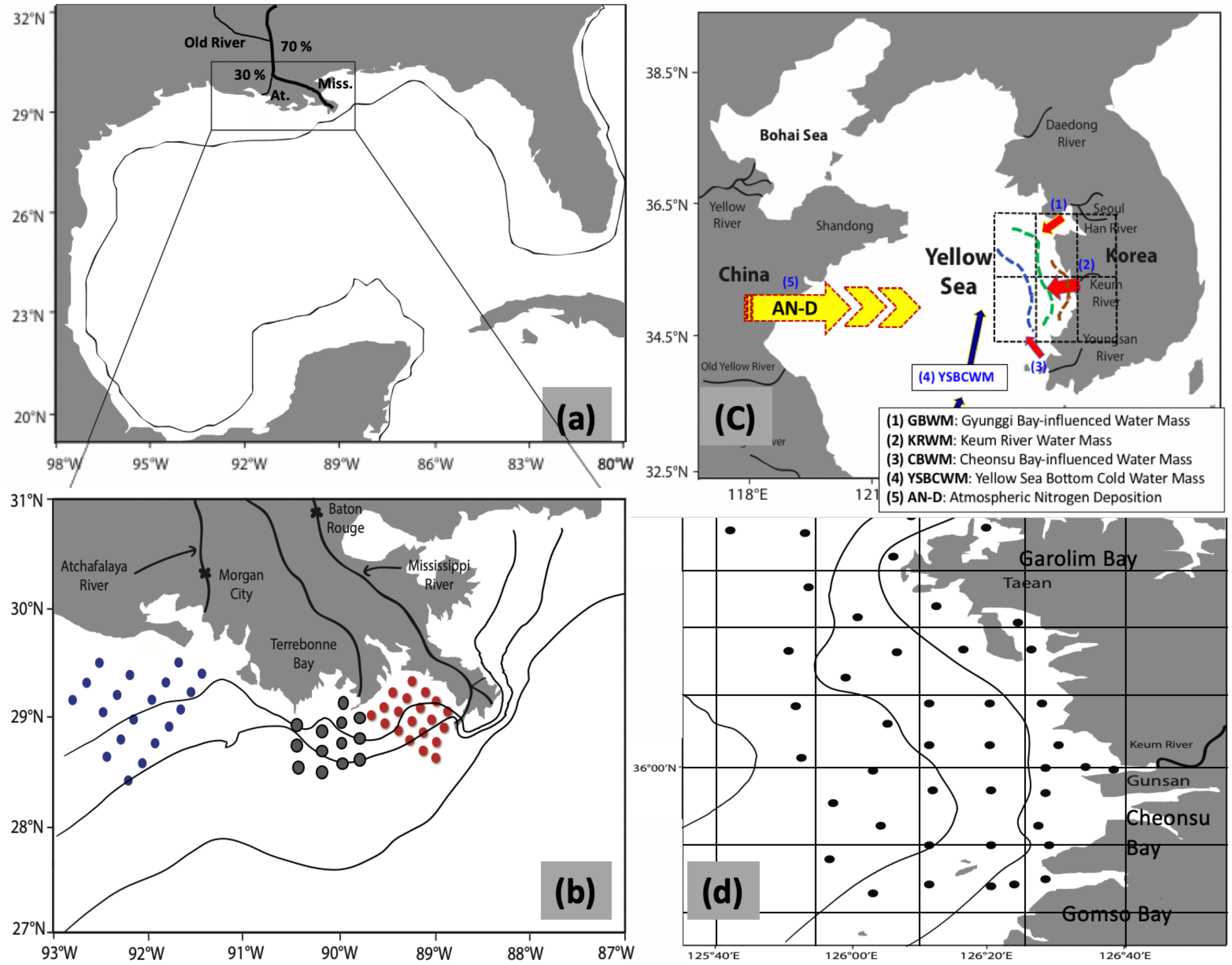

Figure 1. Study sites and sampling areas in the GOM and Korea. Figure (a) shows the sampling area within the northern GOM, and (b) shows station positions from March 2005. Note that MCH project data are widely distributed across the region. Figure (c) shows the sampling area off the west coast of Korea and (d) shows all of the station positions.

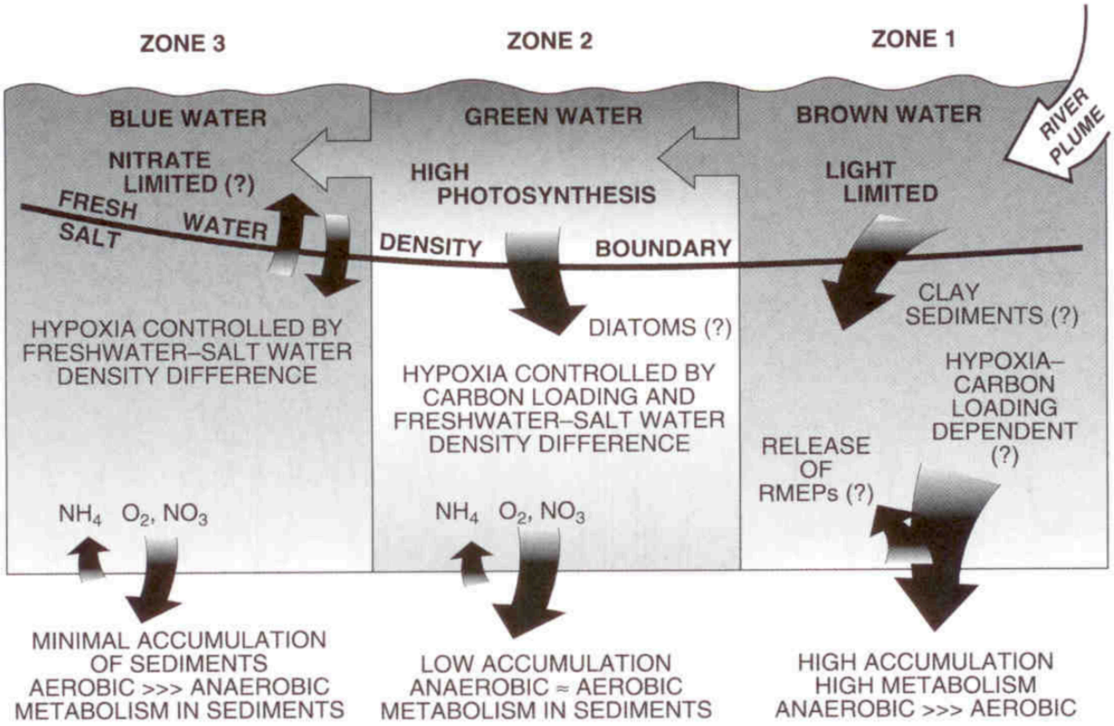

Figure 2. The Rowe and Chapman three zone hypothesis, which described the physical and biochemical processes that initiate and sustain hypoxia on the Texas-Louisiana Shelf, [Rowe and Chapman, 2002]. *Reprinted with permission of Gulf of Mexico Science.*

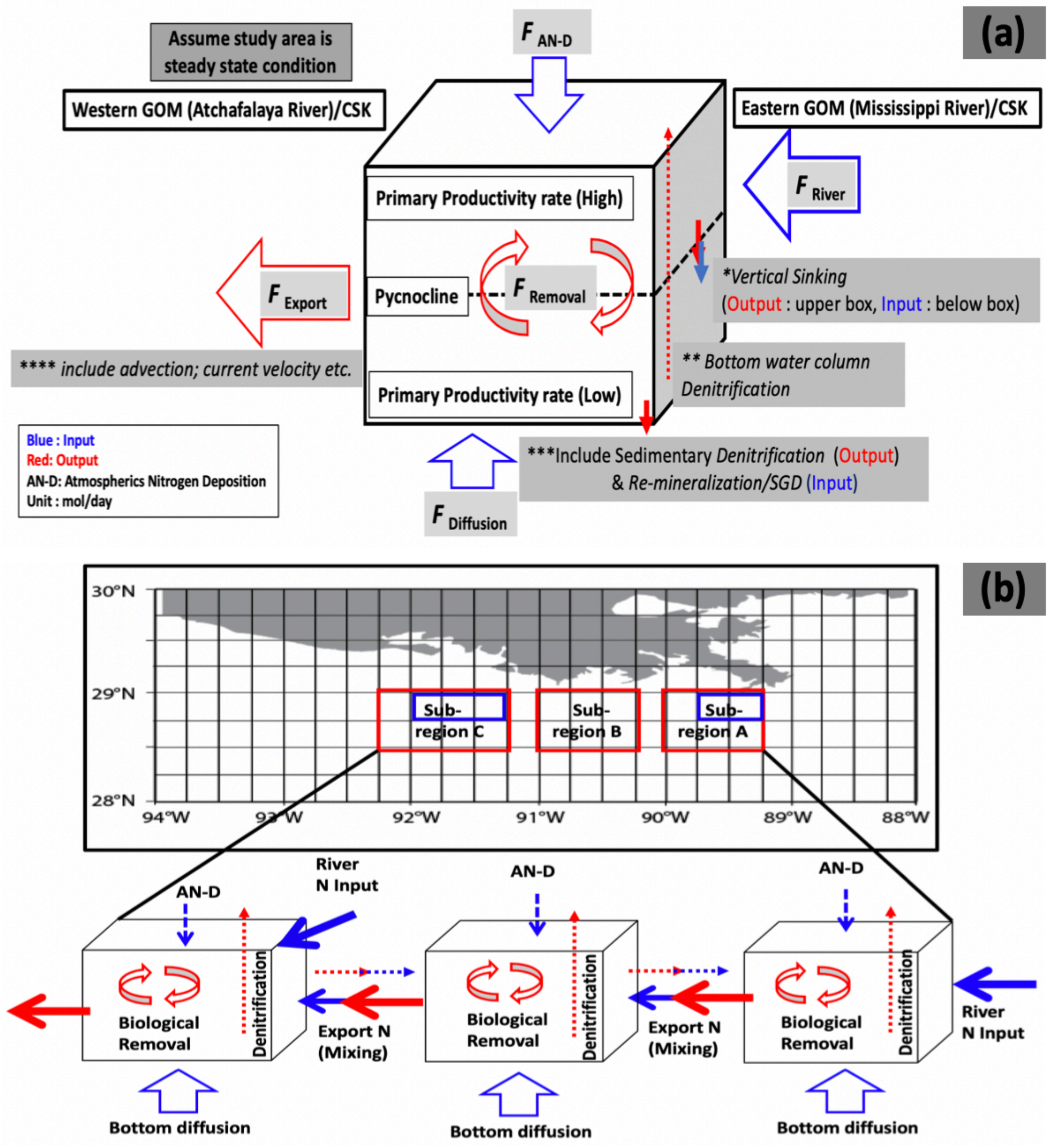

Figure 3. (a) Input (blue) and output (red) sources for each 0.25° box (see text for details); (b) Area of each sub-region (red) and boxes affected by direct riverine input (blue). Export N (Mixing) represents the advective transport term. The processes of biogeochemical and transport processes of both regions are the same and each in/out put factor is the same in the GOM and CSK. Note that transfer between boxes occurs in both directions alongshore and onshore/offshore and is not a one-dimensional process as suggested in the diagram.

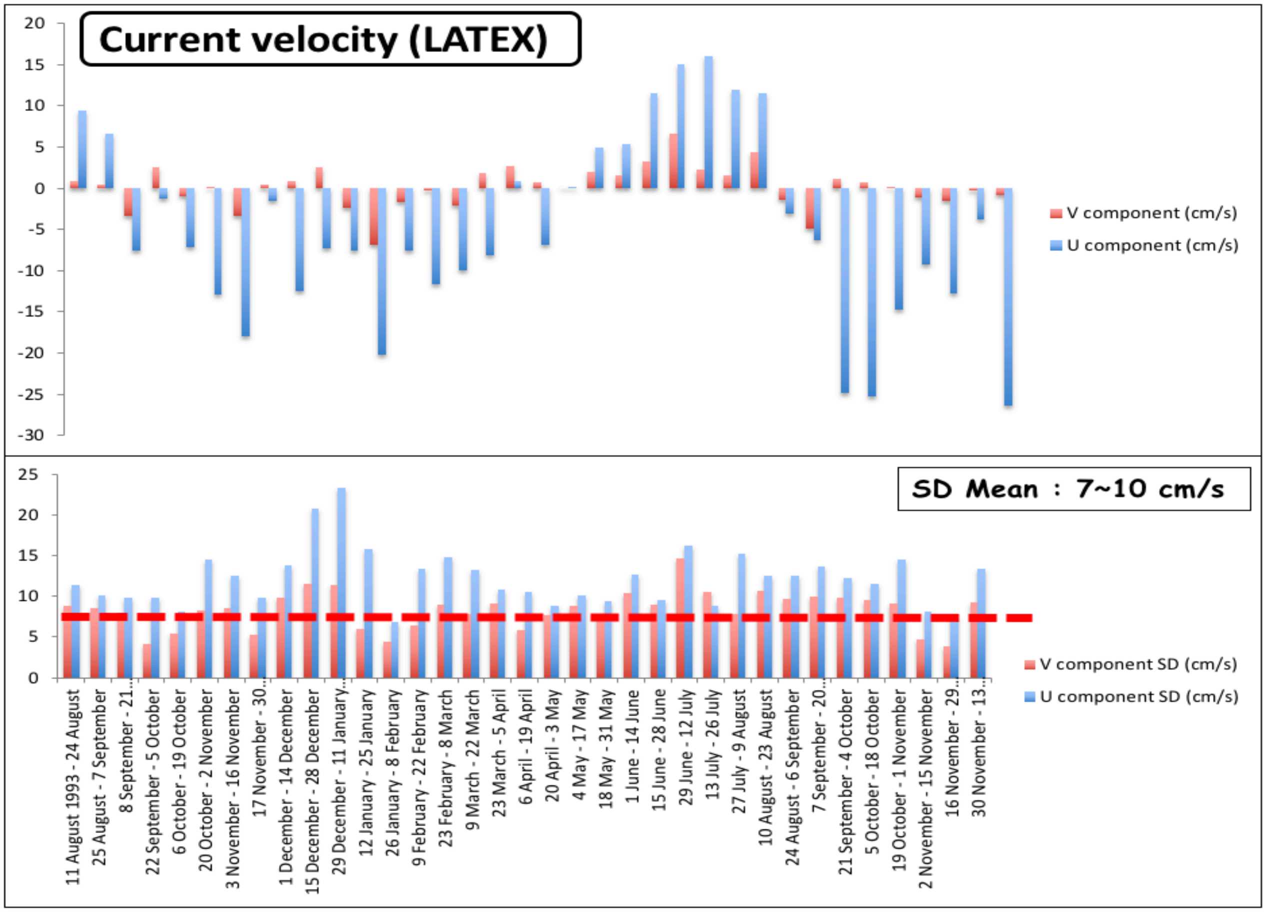

Figure 4. Mean ocean current velocities (a) and standard deviations (b) for biweekly periods from August 1993 through December 1994 based on data from LATEX project. Positive values of U show eastward flow; positive values of V show northward flow.

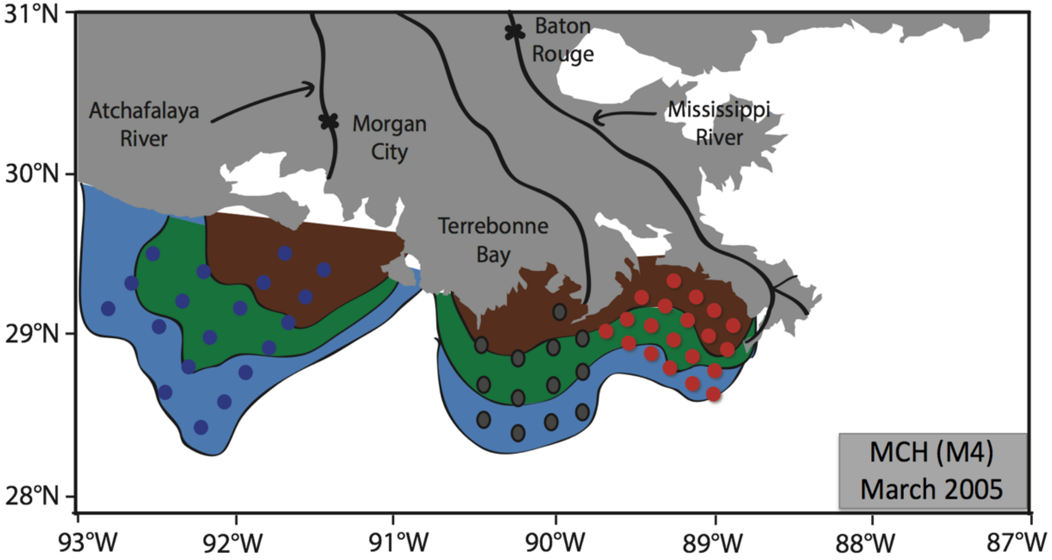

Figure 5. Extent of the three zones defined by RC02 based on the mean concentration of nutrient (DIN) at each station during the MCH M4 cruise in March 2005, showing their correspondence to the three sub-regions used in the box model. Red, grey and blue stations correspond to sub-regions A (near the Mississippi River), B (between the Mississippi and Atchafalaya), and C (near the Atchafalaya) respectively.

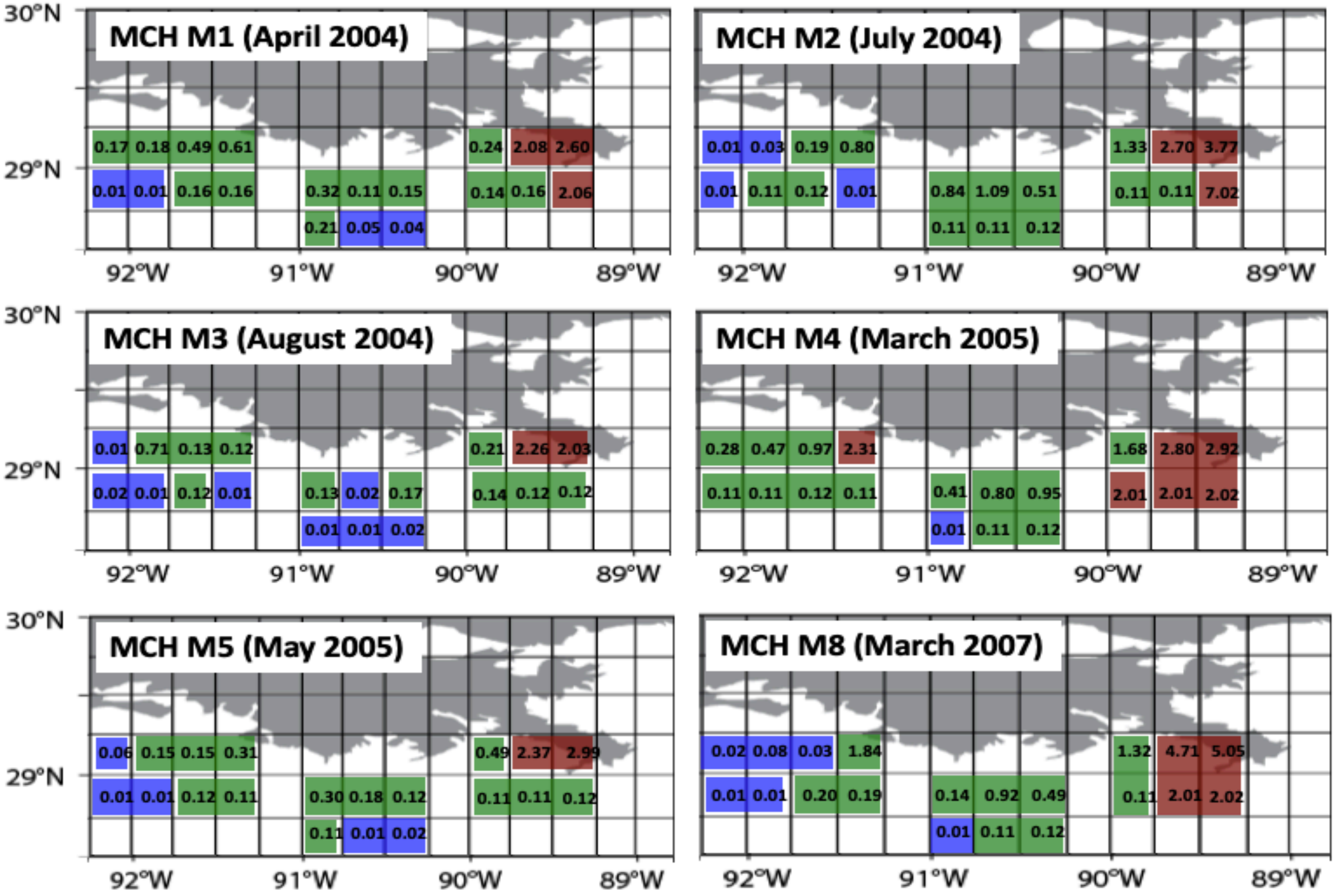

Figure 6a. Areal distributions of the three zones using data from above the pycnocline, based on N-mass balance model results. Colors and numbers represent boxes found in each of the three zones in terms of potential productivity (Unit: gC m^{-2} day^{-1}).

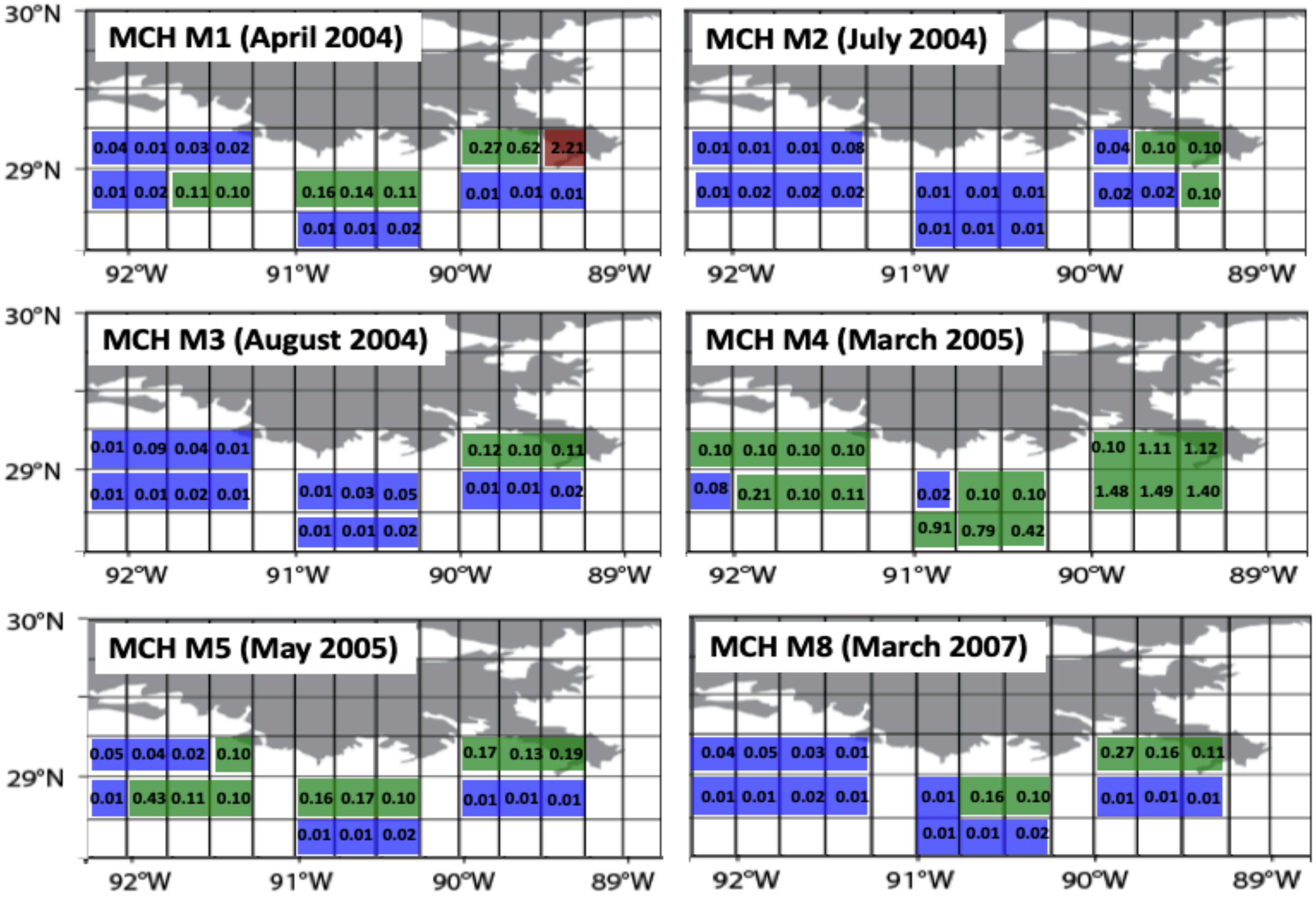

Figure 6b. As for 6a, using data from below the pycnocline.

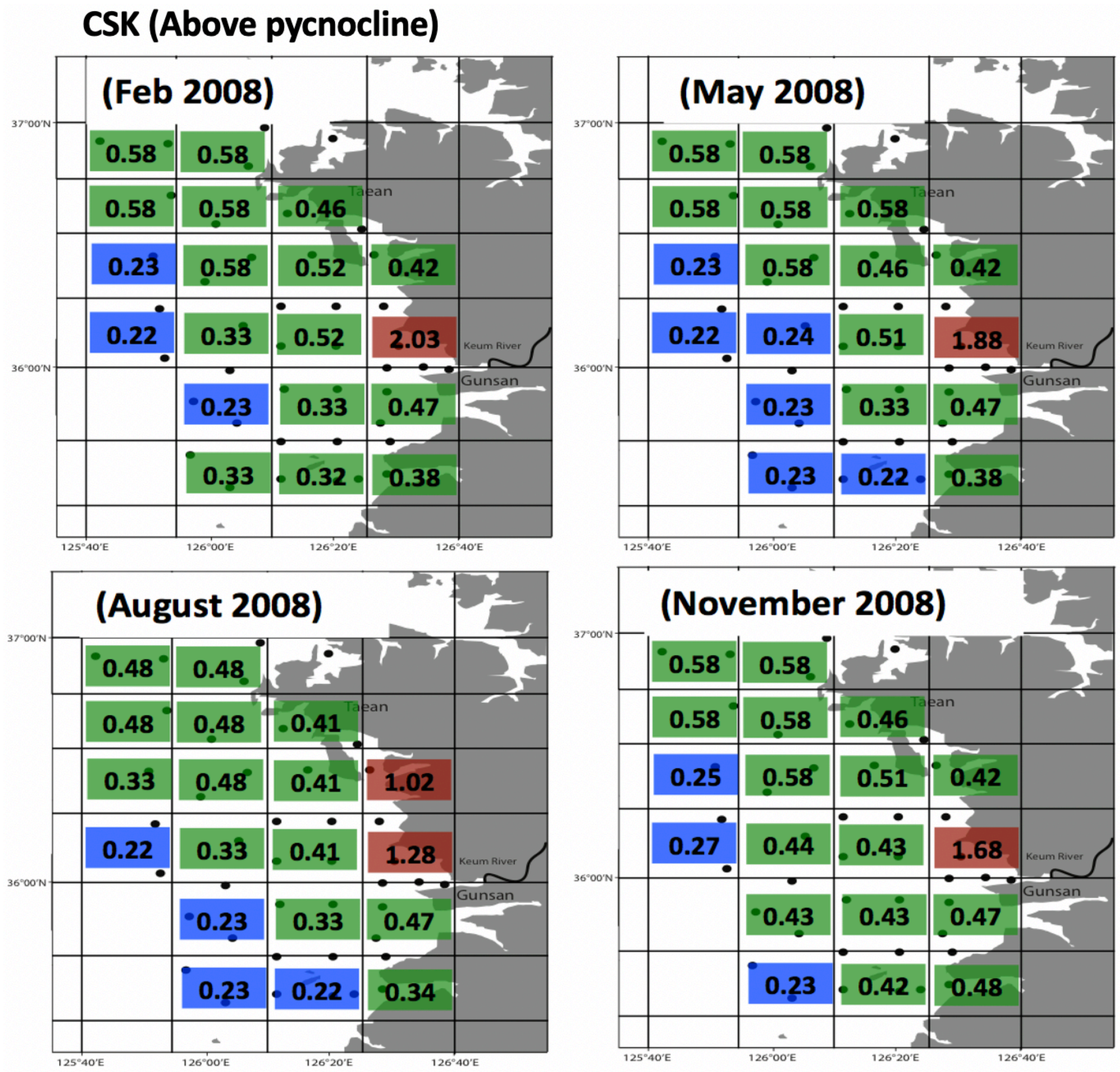

Figure 7a. The distribution of the three zones off Mid-western Korea (CSK) above the pycnocline based on the RC02 hypothesis applied to the N mass balance model. Colors and numbers represent boxes found in each of the three zones in terms of potential productivity (Unit: gC m^{-2} day^{-1}).

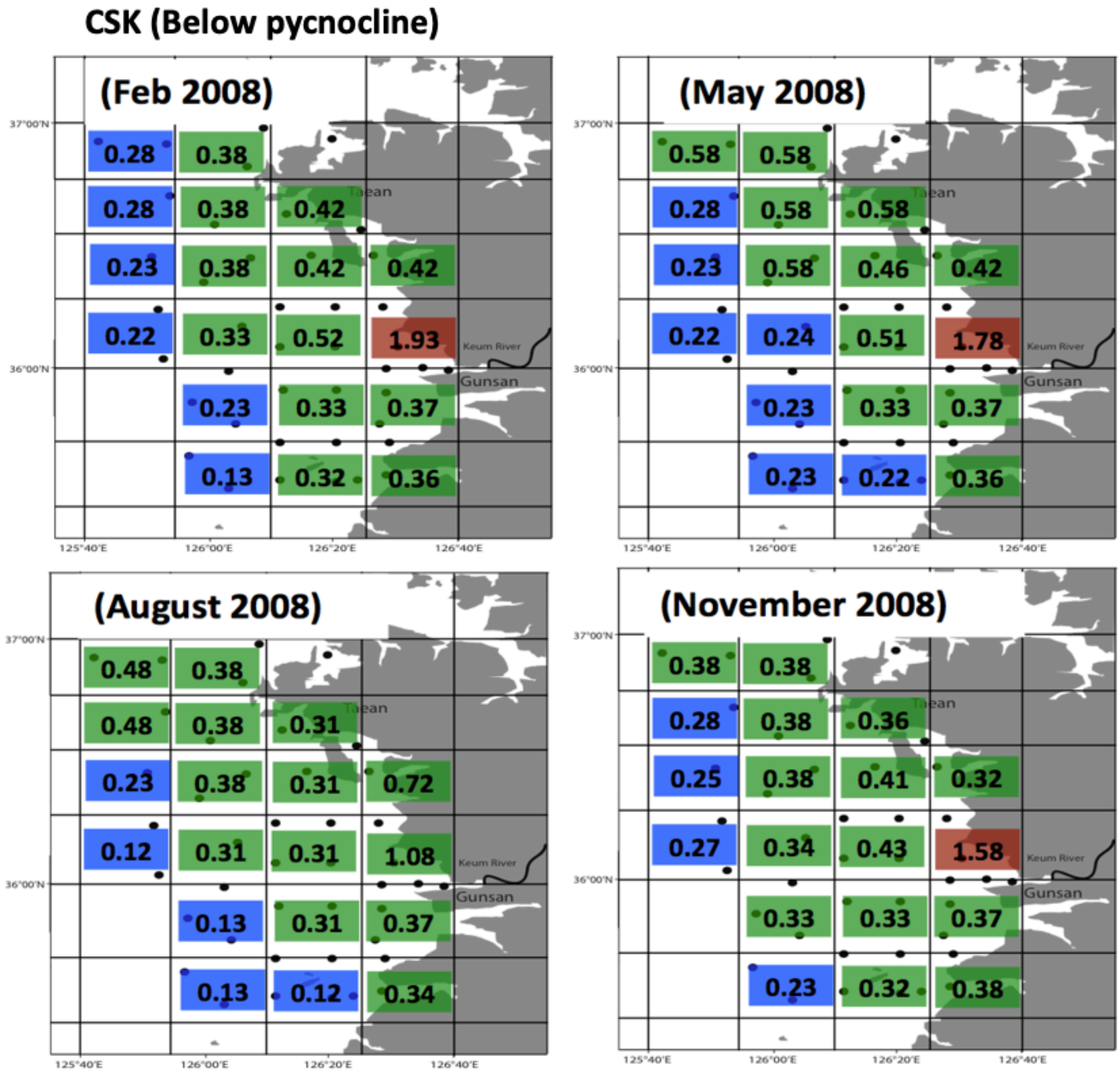

Figure 7b. As for 7a, using data from below the pycnocline.

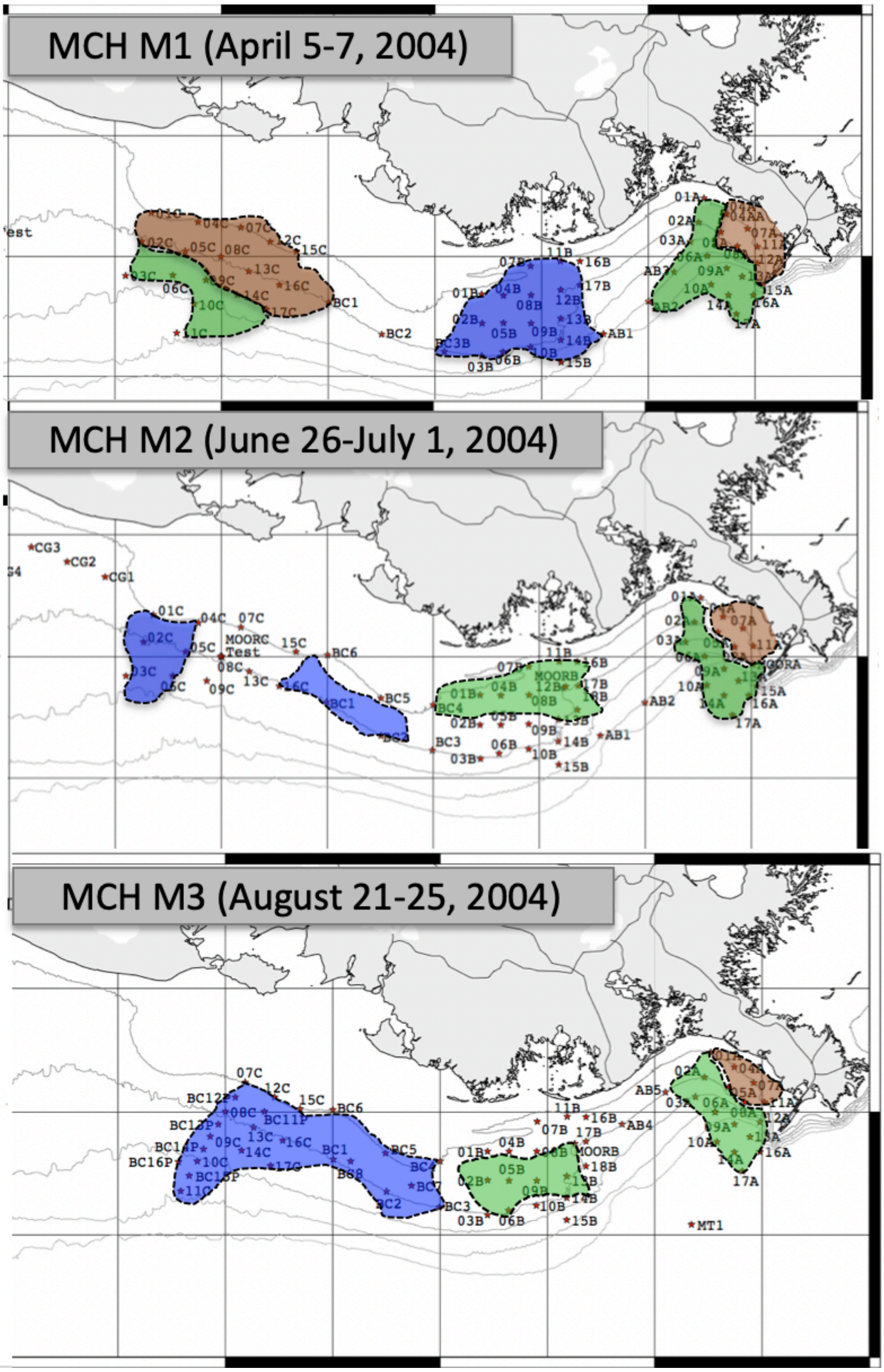

Figure 8. Distribution of the three zones during cruises MCH M1-M3 based on salinity data (Lahiry, 2007). Areas shaded in three colors represent the brown, green and blue zones respectively.

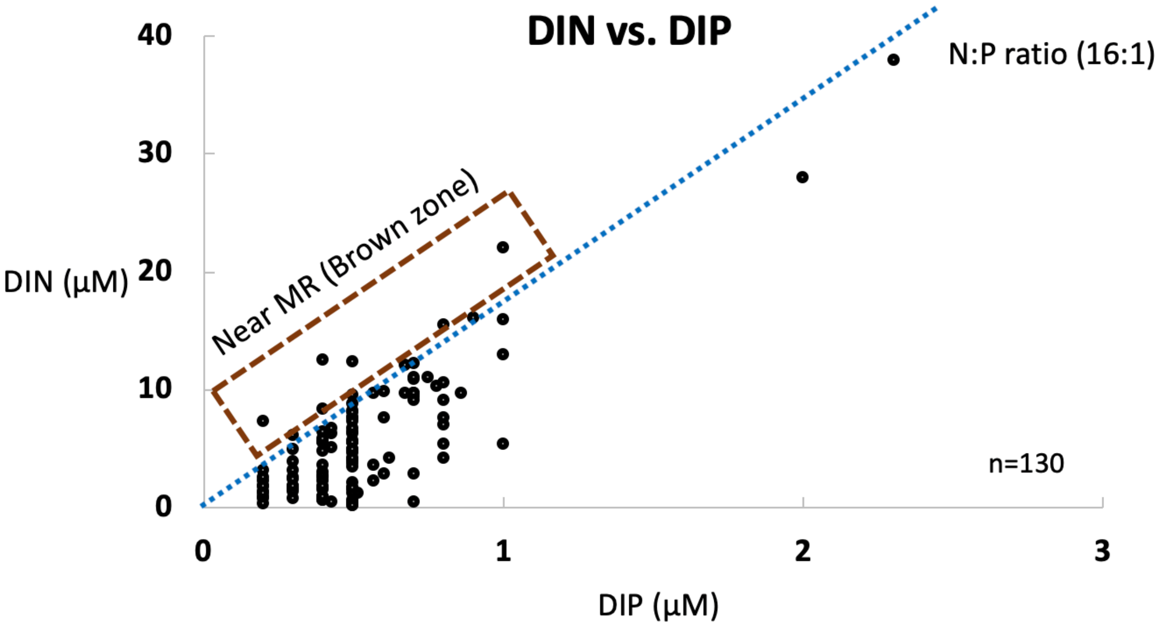

Figure 9. DIN against DIP during sampling periods in the GOM and CSK. Nearly all samples had an N:P ratio of < 16, which indicated potential N-limited condition. At a few points near the brown zone the ratio was between 16 -18; this is where light-limitation is expected according to RC02.

Table 1. Sampling dates for data from Gulf of Mexico projects and the coastal sea of Korea. Winter data are listed for the Gulf of Mexico cruises.

Study area	**Date**	**Cruise number**
Gulf of Mexico MCH	April 5~7, 2004	MCH M1
	June 26~July 1, 2004	MCH M2
	August 21~25, 2004	MCH M3
	March 23~27, 2005	MCH M4
	May 20~26, 2005	MCH M5
	March 23~29, 2007	MCH M8
Korea CSK	Feb, May, Aug, Nov (2008)	

Table 2. Atmospheric Nitrogen Deposition (AN-D) in the USA and in the Yellow Sea.

Watersheds	AN-D (Kg/ha/year)	References
Casco Bay, ME	1.5	Castro and Driscoll. 2002
Merrimack River, MA	1.2 ~ 4.0	Alexander et al. 2000
Long Island Sound, CT	1.8	Castro and Driscoll. 2002
Delaware Bay, DE	2.2 ~ 4.4	Castro and Driscoll. 2002 Goolsby. 2000
Chesapeake Bay	1.4 ~ 17.4	Alexander et al. 2000 Castro, M. S et al. 2000 Castro and Driscoll. 2002 Goolsby. 2000
Gulf of Mexico	10.0 ~ 11.5	Wade and Sweet. 2008
Bohai Sea	64.2 ~ 142.5	Shou et al. 2018
Yellow Sea (China on the west side)	16.1 ~ 18.4 29.9 ~ 32.8 38.1 ~ 92.4	Zhao et al. 2015 Luo et al. 2014 Shou et al. 2018
Yellow Sea (Korea on the east side)	15.0 ~ 58.2	Kim (JY) et al. 2010

Table 3. Definitions and values used in N-mass balance model to calculate DIN removal by biological production. (a) Each one quarter degree box; (b) Wade and Sweet 2008 for GOM region; (c) McCarthy et al., 2015 (d) Lee et al., 2012; (e) McCarthy et al., 2015; (f) Qureshi 1995. *F_{Atmo}^{DIN} of CSK region is used as mean values of Asia data in Table 2, which is initially 5 times higher than that of GOM (1.4 X 10^5 mol day^{-1}). ** The unit of F_{Sink}^{DIN} was converted to mol day^{-1} from the unit of original data (gN m^{-2} day^{-1}) with area of box (0.25 m x 0.25 m) and molar mass of N (14 g mol $^{-1}$). All unit were converted to mol day^{-1} multiplied by area of box (0.25 m x 0.25 m).

Unit	Definitions	Value
A_{Bott} (m^2)	Area of box	6.2 X 10^8 m^2 (a)
C_{Box}^{DIN} (μM)	DIN concentration in each area (box)	
V_S (m^3)	Water volume of box	A_{Bott} X Pycnocline depth
C_{EX}^{DIN} (mmol m^{-3})	Different concentration between each box **C_{EX}= (C_{On} - C_{Off}) or (C_{East} – C_{West}) for DIN**	
λ_{Mix} (day^{-1})	Mixing rate of each box to box (**A reciprocal of the water residence time**)	
F_{River} (day^{-1})	River discharge	
F_{River}^{DIN} (mol day^{-1})	DIN flux from each river discharge	
F_{Atmo}^{DIN} (mol day^{-1})	Diffusive flux from Atmospheric deposition (Bulk N deposition rate x A $_{Bott}$ (A $_{surface\ of\ ocean}$) for DIN	1.4 X 10^5 mol day^{-1} * (b)
F_{Bott}^{DIN} (mol day^{-1})	Benthic flux from the bottom sediments (Net DIN release considered regeneration, groundwater inputs, and uptake of NO_2/ NO_3)	1.2 mmol N m^{-2} day^{-1} (c) 6.2 mmol N m^{-2} day^{-1} (d)
F_{Export}^{DIN} (mol day^{-1})	An advection term which calculated from the current velocity	
F_{Deni}^{DIN} (mol day^{-1})	Denitrification in the water column	2.1 mmol N m^{-2} day^{-1} (e)
F_{Sink}^{DIN} (mol day^{-1})	Vertical sinking of DIN flux from sediment trap data	0.1 ~ 1 gN m^{-2} day^{-1} ** (f)
$F_{Removal}^{DIN}$ (day^{-1})	Removal by biological production (Assuming that the other removal factors are negligible above the pycnocline layer)	

Table 4. Simulation results for selected model scenarios based on MCH M1 (April 5-7, 2004). Biological production is calculated by our N-mass balance model. Oxygen demand is calculated by Redfield stoichiometry ratio (C: O_2 = 106: 138) (Unit: gC m^{-2} day^{-1}).

	F_{River}	$F_{AN\text{-}D}$	$F_{Bott/SGD}$	**Biological production**	**Oxygen demand**
Nominal Value	1.4×10^7 (~98 %)	1.4×10^5 (~1 %)	1.4×10^5 (~1 %)	Base line	
Scenario 1	5.6×10^6 (~93 %)	2.8×10^5 (~5%)	1.4×10^5 (~2%)	~45% decreased	~58% decreased
Scenario 2	9.8×10^6 (~96 %)	2.8×10^5 (~3%)	1.4×10^5 (~1%)	~22% decreased	~28% decreased
Scenario 3	1.7×10^7 (~97 %)	2.8×10^5 (~2%)	1.4×10^5 (~1%)	~17% increased	~21% increased

Table 5. Simulation results for selected model scenarios based on CSK (February 2008) data. Biological production is calculated by our N-mass balance model. Oxygen demand is calculated by the Redfield stoichiometry ratio (C: O_2 = 106: 138) (Unit: gC m-2 day-1).

	F_{River}	$F_{AN\text{-}D}$	$F_{Bott/SGD}$	**Biological production**	**Oxygen demand**
Nominal Value	1.9×10^6 (~60%)	6.0×10^5 (~20%)	6.0×10^5 (~20%)	Base line	
Scenario 1	7.2×10^5 (~29%)	1.2×10^6 (~47%)	6.0×10^5 (~24%)	~13% decreased	~16% decreased
Scenario 2	1.3×10^6 (~41%)	1.2×10^6 (~39%)	6.0×10^5 (~20%)	~2% decreased	~2% decreased
Scenario 3	2.2×10^6 (~55%)	1.2×10^6 (~30%)	6.0×10^5 (~15%)	~25% increased	~32% increased